"Continuum Solvation Models,"
C. J. Cramer and D. G. Truhlar,
in *Solvent Effects and Chemical Reactivity*,
edited by O. Tapia and J. Bertrán
(Kluwer, Dordrecht, 1996), pp. 1–80.

Continuum Solvation Models

Christopher J. Cramer and Donald G. Truhlar
Department of Chemistry and Supercomputer Institute, University of Minnesota, 207 Pleasant St. SE, Minneapolis, MN 55455-0431

MANUSCRIPT COMPLETED JUNE 30, 1995

Abstract This chapter reviews the theoretical background for continuum models of solvation, recent advances in their implementation, and illustrative examples of their use. Continuum models are the most efficient way to include condensed-phase effects into quantum mechanical calculations, and this is typically accomplished by the using self-consistent reaction field (SCRF) approach for the electrostatic component. This approach does not automatically include the non-electrostatic component of solvation, and we review various approaches for including that aspect. The performance of various models is compared for a number of applications, with emphasis on heterocyclic tautomeric equilibria because they have been the subject of the widest variety of studies. For nonequilibrium applications, e.g., dynamics and spectroscopy, one must consider the various time scales of the solvation process and the dynamical process under consideration, and the final section of the review discusses these issues.

Contents

1 Introduction

Accurate treatments of condensed-phase systems are particularly challenging for theoretical chemistry. The primary reason that condensed-phase problems are formidable is the intractability of solving the Schrödinger equation for large, non-periodic systems. Although the nuclear degrees of freedom may be rendered separable from the electronic ones by invocation of the Born-Oppenheimer approximation, the electronic degrees of freedom remain far too numerous to be handled practically, especially if a quantum mechanical approach is used without compromise. Therefore it is very common to replace the quantal problem by a classical one in which the electronic energy plus the coulombic interactions of the nuclei, taken together, are modeled by a classical force field—this approach is usually called molecular mechanics (MM). Another approach is to divide the system into two parts: (1) the primary subsystem consisting of solute and perhaps a few nearby solvent molecules and (2) the secondary subsystem consisting of the rest. The primary subsystem might be treated by quantum mechanics to retain the accuracy of that approach, whereas the secondary subsystem, for all practical purposes, is treated by MM to reduce the computational complexity. Such hybrids of quantum mechanics and classical mechanics, often abbreviated QM/MM, allow the prediction of properties dependent on the quantal nature of the solute, which is especially important for conformational equilibria dominated by stereoelectronic effects, open shell systems, bond rearrangements, and spectroscopy. At the same time, this approach permits the treatment of specific first-solvation-shell interactions.

The QM/MM methodology [1-7] has seen increasing application [8-16] and has been recently reviewed [17-19]. The classical solvent molecules may also be assigned classical polarizability tensors, although this enhancement appears to have been used to date only for simulations in which the solute is also represented classically [20-30]. The treatment of the electronic problem, whether quantal, classical, or hybrid, eventually leads to a potential energy surface governing the nuclear coordinates.

The treatment of the nuclear coordinates also presents imposing challenges. The potential energy hypersurface for a condensed-phase system has numerous low-energy local minima. An accurate prediction of thermodynamic and quasi-thermodynamic properties thus requires wide sampling of the $6N$-dimensional energy/momentum phase space, where N is the number of particles [31, 32]. Both dynamical and probabilistic methods may be employed to accomplish this sampling [33-44], but it can be difficult to converge [42, 45-50], and it is expensive when long-range forces (e.g., Coulomb interactions) are

significant [48, 51-54]. Often local minima in the hypersurface have steep surrounding potentials due to intermolecular interactions or to solute molecules having multiple conformations separated by significant barriers [48, 55]; such situations are problematic for sampling approaches that are easily trapped in deep potential wells. The (impractical) fully quantal approach, and the QM/MM and fully MM methods that treat solvent molecules explicitly, share the disadvantage that they all require efficient techniques for the sampling of phase space. For the QM/MM and fully MM approaches, this sampling problem becomes the computational bottleneck.

When structural and dynamical information about the solvent molecules themselves is not of primary interest, the solute-solvent system may be made simpler by modeling the secondary subsystem as an infinite (usually isotropic) medium characterized by the same dielectric constant as the bulk solvent, i.e., a dielectric continuum. In most applications the continuum may be thought of as a configuration-averaged or time-averaged solvent environment, where the averaging is Boltzmann weighted at the temperature of interest. The dielectric continuum approach is thus also sometimes referred to as a "mean-field" approach. The model includes polarization of the dielectric continuum by the solute's electric field; that polarization and the energetics of the solute-continuum interaction are calculated by classical electrostatic formulas [56], in particular the Poisson equation or the Poisson-Boltzmann equation, the latter finding use in systems where the continuum is considered to have an ionic strength arising from dissolved salts.

Continuum models remove the difficulties associated with the statistical sampling of phase space, but they do so at the cost of losing molecular-level detail. In most continuum models, dynamical properties associated with the solvent and with solute-solvent interactions are replaced by equilibrium averages. Furthermore, the choice of where the primary subsystem "ends" and the dielectric continuum "begins", i.e., the boundary and the shape of the "cavity" containing the primary subsystem, is ambiguous (since such a boundary is intrinsically non-physical). Typically this boundary is placed on some sort of van der Waals envelope of either the solute or the solute plus a few key solvent molecules.

Continuum models have a long and honorable tradition in solvation modeling; they ultimately have their roots in the classical formulas of Mossotti (1850), Clausius (1879), Lorentz (1880), and Lorenz (1881), based on the polarization fields in condensed media [32, 57]. Chemical thermodynamics is based on free energies [58], and the modern theory of free energies in solution is traceable to Born's derivation (1920) of the electrostatic free energy of insertion of a monatomic ion in a continuum dielectric [59], and Kirkwood and Onsager's

closely related treatments [60-62] (1930s) of the electrostatic free energy of insertion of dipolar solutes. The seminal idea of a reaction field [32] was developed in this work. Nonelectrostatic contributions to solvation were originally treated by molecular models. However, Lee and Richards [63] and Hermann [64] introduced the concept of the solvent accessible surface area (SASA). When a proportionality is assumed between, on the one hand, the SASA and, on the other hand, non-bulk-type electrostatic effects and non-electrostatic effects in the first solvation shell (where they are largest), this augments the continuum approach in a rational way. The quasithermodynamic formulation of transition state theory extends all these concepts to the treatment of reaction rates by defining the condensed-phase free energy of activation [65-67]. The breakdown of transition state theory for dynamics, which is related to (if not identical to) the subject of nonequilibrium solvation, can also be discussed in terms of continuum models, as pioneered in Kramers' model involving solvent viscosity [67-69] and in Marcus' work involving nonequilibrium polarization fields [70].

The last thirty years have seen a flowering of simulation techniques based on explicit treatments of solvent molecules (some references are given above). Such methods provide new insight into the reasons why continuum methods work or don't work. However they have not and never will replace continuum models. In fact, continuum models are sometimes so strikingly successful that hubris may be the most serious danger facing their practitioners. One of the goals of this present chapter will be to diffuse (but not entirely deflate!) any possible overconfidence.

The present chapter thus provides an overview of the current status of continuum models of solvation. We review available continuum models and computational techniques implementing such models for both electrostatic and non-electrostatic components of the free energy of solvation. We then consider a number of case studies, with particular focus on the prediction of heterocyclic tautomeric equilibria. In the discussion of the latter we center attention on the subtleties of actual chemical systems and some of the dangers of applying continuum models uncritically. We hope the reader will emerge with a balanced appreciation of the power and limitations of these methods.

At this point we note the existence of several classic and recent reviews devoted to, or with considerable attention paid to, continuum models of solvation effects, and we direct the reader to these works [71-83] for other perspectives that we consider complementary to what is presented here.

Section 2 presents a review of the theory underlying self-consistent continuum models, with section 2.1 devoted to electrostatics and section 2.2 devoted to the incorporation of non-electrostatic effects into continuum solvation

modeling. Section 3 discusses the various algorithmic implementations extant. Section 4 reviews selected applications to various equilibrium properties and contrasts different approaches. Section 5 offers a brief overview of methods to extend continuum solvation modeling to account for dynamic effects in kinetics and spectroscopy, and Section 6 closes with some conclusions and remarks about future directions.

2 Theory

2.1 ELECTROSTATICS

A charged system has an electrical potential energy equal to the work that must be done to assemble it from separate components infinitely far apart and at rest. This energy resides in and can be calculated from the electric field. This electrostatic potential energy, when considered as a thermodynamic quantity, is a free energy because it is the maximum work obtainable from the system under isothermal conditions [84]. We have the option, therefore, of calculating it as an electrostatic potential energy or as the isothermal work in a charging process. Although the latter approach is very popular, dating back to its use by Born, the former approach seems to provide more insight into the quantum mechanical formulation, and so we adopt that approach here. Recognizing that the electrostatic potential energy is the free energy associated with the electric polarization of the dielectric medium, we will call it G_P.

In general the electrostatic potential energy of a charge distribution in a dielectric medium is [84, 85]

$$G_P = \frac{1}{2}\int d\mathbf{r}\left[\mathbf{E}^T(\mathbf{r})\mathbf{D}(\mathbf{r}) - 4\pi\mathbf{D}^T(\mathbf{r})\mathbf{D}(\mathbf{r})\right] \tag{1}$$

where the integration is over the whole dielectric medium (in the case of solvation this means an integration over all space except that occupied by the solute), **E** is the electric field, T denotes a transpose, **D** is the dielectric displacement, and the second term in the integrand references the energy to that for the same solute in a vacuum. Recall from electrostatics that

$$\nabla \cdot \mathbf{D} = \rho_{free} \tag{2}$$

where ρ_{free} is the charge density of the material inserted into the dielectric, i.e., of the solute, but

$$\nabla \cdot \mathbf{E} = 4\pi\rho_{\text{total}} \tag{3}$$

where

$$\rho_{\text{total}} = \rho_{\text{free}} + \rho_{\text{P}} \tag{4}$$

and ρ_{P} is the polarization charge density, i.e., the charge density induced in the dielectric medium by the solute (in classical electrostatics, ρ_{P} is often called ρ_{bound}). In an isotropic medium, assuming linear response of the solvent to the solute, it is generally the case that [84]

$$\mathbf{E}(\mathbf{r}) = \frac{4\pi}{\varepsilon(\mathbf{r})}\mathbf{D}(\mathbf{r}) \tag{5}$$

where $\varepsilon(\mathbf{r})$ is the dielectric constant (i.e., relative permittivity) of the solvent at position $\mathbf{r}$.

Clearly, $\mathbf{D}(\mathbf{r})$ is a function of the solute charge density only, and we can write

$$\mathbf{D}(\mathbf{r}) = \langle\psi|\mathbf{d}(\mathbf{r})|\psi\rangle \tag{6}$$

where $\mathbf{d}(\mathbf{r})$ is the operator that generates the displacement at $\mathbf{r}$. Then

$$G_{\text{P}} = \frac{1}{2}\int d\mathbf{r}\left[\mathbf{E}^{\text{T}}(\mathbf{r}) - 4\pi\mathbf{D}^{\text{T}}(\mathbf{r})\right]\langle\psi|\mathbf{d}(\mathbf{r})|\psi\rangle. \tag{7}$$

Using the linear response result (5), we then get

$$G_{\text{P}} = -2\pi\int d\mathbf{r}\left[1 - \frac{1}{\varepsilon(\mathbf{r})}\right]\langle\psi|\mathbf{d}^{\text{T}}(\mathbf{r})|\psi\rangle\langle\psi|\mathbf{d}(\mathbf{r})|\psi\rangle \tag{8a}$$

$$= \left\langle\psi\left|-2\pi\int d\mathbf{r}\left[1 - \frac{1}{\varepsilon(\mathbf{r})}\right]\mathbf{d}^{\text{T}}(\mathbf{r})\langle\psi|\mathbf{d}(\mathbf{r})|\psi\rangle\right|\psi\right\rangle \tag{8b}$$

$$= \langle\psi|G_{\text{P,op}}|\psi\rangle \tag{8c}$$

where

$$G_{\mathrm{P,op}}|\psi\rangle = -\frac{1}{2} K_{\mathrm{op}}\, \mathbf{d}^{\mathrm{T}}(\mathbf{r}) \langle \psi | \mathbf{d}(\mathbf{r}) | \psi \rangle | \psi \rangle \tag{9}$$

and we have defined the integral operator

$$K_{\mathrm{op}} f(\mathbf{r}) \equiv 4\pi \int d\mathbf{r}' \left(1 - \frac{1}{\varepsilon(\mathbf{r}')} \right) f(\mathbf{r}') \tag{10}$$

for any function $f(\mathbf{r})$. If the gas-phase Hamiltonian is H_0, then the solute's energy in the electrostatic field of the polarized solvent is

$$G_{\mathrm{ENP}} = \langle \psi | H_0 + G_{\mathrm{P,op}} | \psi \rangle \tag{11}$$

where G_{ENP} has the thermodynamic interpretation of the total internal energy of the solute (represented by H_0) plus the electric polarization free energy of the entire solute-solvent system.

We note that G_{ENP} is a complicated function of ψ; in particular it is nonlinear. Recall that an operator L_{op} is linear if

$$L_{\mathrm{op}} | c_1 \psi_1 + c_2 \psi_2 \rangle = c_1 L_{\mathrm{op}} | \psi_1 \rangle + c_2 L_{\mathrm{op}} | \psi_2 \rangle . \tag{12}$$

However

$$G_{\mathrm{P,op}} | \psi_1 + \psi_2 \rangle = -\frac{1}{2} K_{\mathrm{op}}\, \mathbf{d}^{\mathrm{T}}(\mathbf{r}) \langle \psi_1 + \psi_2 | \mathbf{d}(\mathbf{r}) | \psi_1 + \psi_2 \rangle | \psi_1 \rangle$$

$$-\frac{1}{2} K_{\mathrm{op}}\, \mathbf{d}^{\mathrm{T}}(\mathbf{r}) \langle \psi_1 + \psi_2 | \mathbf{d}(\mathbf{r}) | \psi_1 + \psi_2 \rangle | \psi_2 \rangle \tag{13a}$$

$$\neq G_{\mathrm{P,op}} | \psi_1 \rangle + G_{\mathrm{P,op}} | \psi_2 \rangle . \tag{13b}$$

Hence $G_{\mathrm{P,op}}$ is nonlinear, and therefore the energy functional G_{ENP} of (11) is nonlinear.

Note that $G_{\mathrm{P,op}}$ of eq. (9) can be written in several equivalent but different looking forms, as is typical of electrostatic quantities in general. For example, it is often convenient to express the results in terms of the electrostatic scalar potential $\phi(\mathbf{r})$ instead of the electric vector field $\mathbf{E}(\mathbf{r})$. In the formulation above, the dielectric displacement vector field associated with the solute charge distribution induces an electric vector field, with which it interacts. In the electrostatic

potential formulation, the solute charge distribution induces an electrostatic scalar potential field, with which it interacts. The difference between *either* induced field in the presence of solvent compared to the absence of solvent may be called the reaction field, using the language mentioned above as introduced by Onsager. In any such formulation, $G_{P,op}$ will remain nonlinear. In particular it will have the form $A_{op}(\psi^*\psi)$ where A_{op} is some operator. Sanhueza et al. [86] have constructed variational functions representing general nonlinear Hamiltonians having the form $L_{op} + A_{op}(\psi^*\psi)^q$, where q is any positive number. The sense of the notation is simply that ψ^* and ψ each appear to the first power in one term of the operator. Thus, comparing to eq. (9), we see that their treatment reduces to our case when $q = 1$. The $q = 1$ case is of special interest since it arises any time a solute is immersed in a medium exhibiting linear response to it. Since this case is central to the work reviewed in this chapter, we present below a self-contained variational formulation for the $q = 1$ case. In particular we will consider the case of G_{ENP} as expressed above although the procedure is valid for any Hamiltonian whose nonlinearity may be written as $A_{op}(\psi^*\psi)^q$ with $q = 1$.

In order to motivate the quantum mechanical treatment of a system with the energy functional G_{ENP}, we first consider the functional

$$E = \langle \psi | H_0 | \psi \rangle \tag{14}$$

where H_0 is the gas-phase Hamiltonian. We use Euler-Lagrange theory to find a differential equation satisfied by the ψ that extremizes the value of the integral functional E of ψ. The Euler equation for an extremum of E subject to the constraint

$$\langle \psi | \psi \rangle = 1 \tag{15}$$

is

$$\delta\left[E + \lambda\langle \psi | \psi \rangle\right] = 0 \tag{16}$$

where λ is a Lagrange multiplier. Carrying out the variation gives

$$\langle \delta\psi | H_0 | \psi \rangle + \langle \psi | H_0 | \delta\psi \rangle + \lambda\left(\langle \delta\psi | \psi \rangle + \langle \psi | \delta\psi \rangle\right) = 0 \tag{17}$$

or

$$J = 0 \tag{18}$$

where

$$J = 2\Big(\langle \delta\psi | H_0 | \psi \rangle + \lambda \langle \delta\psi | \psi \rangle\Big). \tag{19}$$

For this to be valid for any variation $\delta\psi$, it is required that

$$H_0\psi = -\lambda\psi \tag{20}$$

where λ is evaluated by using eq. (15). To use eq. (15), note that (20) implies that

$$\langle \psi | H_0 | \psi \rangle + \lambda \langle \psi | \psi \rangle = 0 \tag{21}$$

and using (15) then yields the interpretation of λ

$$\lambda = -\langle \psi | H_0 | \psi \rangle = -E. \tag{22}$$

Putting this in (20) yields

$$H_0\psi - E\psi = 0. \tag{23}$$

Thus, as expected, the Euler equation equivalent to extremizing E is the Schrödinger equation.

Now consider the functional

$$G_{\mathrm{ENP}} = \langle \psi | H_0 - \frac{1}{2} K_{\mathrm{op}} \mathbf{d}^{\mathrm{T}}(\mathbf{r}) \langle \psi | \mathbf{d}(\mathbf{r}) | \psi \rangle | \psi \rangle. \tag{24}$$

The Euler equation for an extremum of G_{ENP} subject to the constraint

$$\langle \psi | \psi \rangle = 1 \tag{25}$$

is

$$\delta\left[G_{\mathrm{ENP}} + \lambda \langle \psi | \psi \rangle\right] = 0 \tag{26}$$

where λ is a Lagrange multiplier. Carrying out the variation gives

$$\begin{aligned} J + 2\langle \delta\psi | - \frac{1}{2} K_{\mathrm{op}} \mathbf{d}^{\mathrm{T}}(\mathbf{r}) \langle \psi | \mathbf{d}(\mathbf{r}) | \psi \rangle | \psi \rangle \\ + 2\langle \psi | - \frac{1}{2} K_{\mathrm{op}} \mathbf{d}^{\mathrm{T}}(\mathbf{r}) \langle \delta\psi | \mathbf{d}(\mathbf{r}) | \psi \rangle | \psi \rangle = 0. \end{aligned} \tag{27}$$

For this is to be valid for arbitrary variations $\delta\psi$, it is required that

$$H_0\psi + \lambda\psi - K_{op}\mathbf{d}^T(\mathbf{r})\langle\psi|\mathbf{d}(\mathbf{r})|\psi\rangle\psi = 0 \tag{28}$$

where λ is again to be evaluated from the constraint equation. Following the same procedure as before we find

$$\lambda = -\langle\psi|H_0 - K_{op}\,\mathbf{d}^T(\mathbf{r})\langle\psi|\mathbf{d}(\mathbf{r})|\psi\rangle|\psi\rangle. \tag{29}$$

It is conventional to rewrite eq. (28) as a nonlinear Schrödinger equation with eigenvalue E:

$$\left[H_0 - K_{op}\,\mathbf{d}^T(\mathbf{r})\langle\psi|\mathbf{d}(\mathbf{r})|\psi\rangle - E\right]|\psi\rangle = 0. \tag{30}$$

Comparison of (30) to (28) and (29) shows that

$$E = \langle\psi|H_0 - K_{op}\,\mathbf{d}^T(\mathbf{r})\langle\psi|\mathbf{d}(\mathbf{r})|\psi\rangle|\psi\rangle$$

$$= \langle\psi|H_0|\psi\rangle + 2G_P. \tag{31}$$

Solving the nonlinear Schrödinger equation yields E and ψ and the desired physical quantity G_{ENP} may then be calculated directly from (11) or from

$$G_{ENP} = E + \frac{1}{2}K_{op}\,\mathbf{d}^T(\mathbf{r})\langle\psi|\mathbf{d}(\mathbf{r})|\psi\rangle$$

$$= E - G_P \tag{32}$$

which is easily derived by comparing eq. (8), (9), (24), and (31).

The fact that the eigenvalue E of the nonlinear effective Hamiltonian,

$$H_{eff} = H_0 - K_{op}\,\mathbf{d}^T(\mathbf{r})\langle\psi|\mathbf{d}(\mathbf{r})|\psi\rangle \tag{33}$$

does not equal the expectation value of the functional G_{ENP} that is extremized is sometimes a source of confusion for those unfamiliar with nonlinear Schrödinger equations. This is presumably because in the linear case the expectation value of the function extremized, e.g., eq. (14), and the eigenvalue, e.g., $-\lambda$ in eq. (20), are the same.

The second term of equation (33) may be called the self-consistent reaction field (SCRF) equation in that eq. (30) must be solved iteratively until the

$|\psi>$ obtained by solving the equation is consistent with the $|\psi>$ used to calculate the reaction field. Having established an effective nonlinear Hamiltonian, one may solve the Schrödinger equation by any standard (or nonstandard) manner. The common element is that the electrostatic free energy term G_P is combined with the gas-phase Hamiltonian H_0 to produce a nonlinear Schrödinger equation

$$(H_0 + 2G_P)\psi = E\psi \tag{34}$$

where ψ is the solute wave function, and the reason that $2G_P$ appears in eq. (34) is explained above, namely that G_P depends on $\psi^*\psi$, and one can show that the variational solution of (34) yields the best approximation to

$$E_S \equiv \langle\psi|H_0 + G_P|\psi\rangle. \tag{35}$$

In most work reported so far, the solute is treated by the Hartree-Fock method (i.e., H_0 is expressed as a Fock operator), in which each electron moves in the self-consistent field (SCF) of the others. The term SCRF, which should refer to the treatment of the reaction field, is used by some workers to refer to a combination of the SCRF nonlinear Schrödinger equation (34) and SCF method to solve it, but in the future, as correlated treatments of the solute becomes more common, it will be necessary to more clearly distinguish the SCRF and SCF approximations. The SCRF method, with or without the additional SCF approximation, was first proposed by Rinaldi and Rivail [87, 88], Yomosa [89, 90], and Tapia and Goscinski [91]. A highly recommended review of the foundations of the field was given by Tapia [71].

When the SCRF method is employed in conjunction with Hartree-Fock theory for the solute, then the Fock operator is given by

$$F = F^{(0)} + 2G_{P,op} \tag{36}$$

where $F^{(0)}$ is the gas-phase Fock operator. Using eq. (9) we can also write this as

$$F = F^{(0)} - K_{op}\mathbf{d}^T(\mathbf{r})\langle\psi|\mathbf{d}(\mathbf{r})|\psi\rangle. \tag{37}$$

There is another widely used method of obtaining the Fock operator, namely to obtain its matrix elements $F_{\mu\nu}$ as the derivative of the energy functional with respect to the density. In our case that yields

$$F_{\mu\nu} = \frac{\partial G_{\mathrm{ENP}}}{\partial P_{\mu\nu}} \tag{38a}$$

$$= F_{\mu\nu}^{(0)} + \frac{\partial G_{\mathrm{P}}}{\partial P_{\mu\nu}} \tag{38b}$$

where $F_{\mu\nu}^{(0)}$ is the matrix element of the gas-phase Fock operator, and $P_{\mu\nu}$ is a matrix element of the density. This method bypasses the nonlinear Schrödinger equation and the nonlinear Hamiltonian, but a moment's reflection on the variational process of eqs. (24)–(30) shows that it yields the same results as eqs. (36) and (37). This too has caused confusion in the literature.

In conclusion, we note that there has recently been considerable interest in including intrasolute electron correlation energy in SCRF theory [77, 92-106]. Further progress in this area will be very important in improving the reliability of the predictions, at least for "small" solutes.

Next we discuss two aspects of the physical interpretation of the SCRF method that are well worth emphasizing: (i) the time scales and (ii) the assumption of linear response.

The natural time scale τ_{elec} of the electronic motion of the solute is $\vartheta(h/\Delta E_1)$ where ϑ denotes "order of", h is Planck's constant, and ΔE_1 is the lowest electronic excitation energy. Assuming a typical order of magnitude of 10^1 eV for ΔE_1 yields $\tau_{\mathrm{elec}} = \vartheta(10^{-16}$ s). The time scale for polarization of the solvent is more complicated. For a polar solvent, orientational polarization is the dominant effect, and it is usually considered to have a time scale of $\vartheta(10^{-12}$ s). Thus the electronic motion of the solute should adjust adiabatically to solvent orientational polarization, and the solvent should "see" the average charge distribution (i.e., the "mean field") of the solute. This argument provides a physical justification for the expectation value in (6) providing the field that induces the solvent polarization, resulting in a net electric field given by (5). We should not forget though that a part of the solvent polarization is electronic in origin. The time scale for solvent electronic polarization is comparable to that for electronic motions in the solute, and the SCRF method is not so applicable for this part. A correct treatment of this part of the polarization effect would require a treatment of electron correlation between solute electrons and solvent electrons, a daunting prospect. This correlation problem has also been discussed from other points of view [107-111].

Tapia, Colonna, and Ángyán [112-114] have presented an alternative justification for the appearance of average solute properties in the SCRF

equations. Their argument is based starting with a wave function for the entire solute-solvent system, then assuming a Hartree product wave function of the form $\Psi_{solute}\Psi_{solvent}$. This allows the "derivation" of a solute-only Schrödinger equation identical to the one derived here. The appearance of the Hartree approximation [115] in the derivation again makes it clear that solute-solvent electron correlation is neglected in the SCRF equations. It also raises the question of exchange repulsion, which is the short-range repulsion between two closed-shell systems due to the Pauli Exclusion Principle. (I.e., if the systems start to overlap, their orbitals must distort to remain orthogonal. This raises the energy, and hence it is a repulsive interaction.) Exchange repulsion between two systems is properly included in the Hartree-Fock approximation but not in the Hartree approximation. The neglect of exchange repulsion is a serious limitation of the SCRF model that prevents it from being systematically improvable with respect to the solute-solvent electron correlation.

The assumption of linear response played a prominent role in the derivation (given above) of the SCRF equations, and one aspect of the physics implied by this assumption is worthy of special emphasis. This aspect is the partitioning of G_P into a solute-solvent interaction part G_{sS} and a intrasolvent part G_{SS}. The partitioning is quite general since it follows entirely from the assumption of linear response. Since classical electrostatics with a constant permittivity is a special case of linear response, it can be derived by any number of classical electrostatic arguments. The result is [114, 116-119]

$$G_{SS} = -\frac{1}{2} G_{sS} \tag{39}$$

and hence

$$G_{sS} = 2G_P \tag{40}$$

and

$$G_{SS} = -G_P. \tag{41}$$

The physical interpretation of these equations is that when the solute polarizes the solvent to lower the solute-solvent interaction energy by an amount G_{sS}, half the gain in free energy is canceled by the work in polarizing the solvent, which raises its own internal energy.

Since these equations are general for a system exhibiting linear response, we can illustrate them by the simplest such system, a harmonic oscillator

(representing the solvent) linearly coupled to an external perturbation (representing the solute). The energy of the system (excluding the internal energy of the solute) is

$$V = \frac{1}{2} ky^2 + gys \tag{42}$$

where k is the oscillator force constant, y is the oscillator coordinate, which is a generalized solvent coordinate, g is the coupling force constant, and s is the solute coordinate. We identify

$$G_P = V \tag{43}$$

$$G_{SS} = \frac{1}{2} ky^2 \tag{44}$$

$$G_{sS} = gys. \tag{45}$$

Now, at equilibrium

$$\frac{\partial V}{\partial y} = 0. \tag{46}$$

Therefore, from the derivative of (42):

$$s = - ky/g. \tag{47}$$

and putting this in (45) yields

$$G_{sS} = -ky^2 \tag{48}$$

Comparison of (48) to (44) agrees with (39).

A subject *not* treated here is the use of distance-dependent effective dielectric constants as a way to take account of the structure in the dielectric medium when a solute is present. This subject has recently been reviewed [120]. In the approaches covered in the present chapter, deviations of the effective dielectric constant from the bulk value may be included in terms of physical effects in the first solvation shell, as discussed in Section 2.2.

As a final topic in this section, we briefly consider the effect of electrolyte concentration on the solvent properties. The linearized Poisson-Boltzmann equation [31, 121] can be used instead of (2) and (3) when the dielectric medium

is a salt solution, and this equation can be solved analytically for the case of a single-point charge Z at the center of a cavity of radius ρ in a solvent of dielectric constant ε. The resulting electric potential at a distance r from the center of the cavity is [122]

$$\phi(r) = \frac{Z}{\varepsilon r} D \frac{\exp[-(r-\rho)/r_D]}{1+\rho/r_D} \tag{49}$$

where r_D is the Debye screening length

$$r_D = 1/\kappa = [\varepsilon RT/(8\pi I)]^{1/2}, \tag{50}$$

R is the gas constant, T the temperature, and I is ionic strength. We may write this as

$$\phi(r) = \frac{Z}{\varepsilon_{\text{eff}}(r) r} \tag{51}$$

which yields [123]

$$\varepsilon_{\text{eff}}(r) = \varepsilon\left(1+\frac{\rho}{r_D}\right)e^{(r-\rho)/r_D} \tag{52}$$

For 0.1 M NaCl in water, this yields $\varepsilon_{\text{eff}}(r)$ values of about 105 and 130 at r equals 3 and 5 Å, respectively, as compared to ε = 78.5 for pure water. Since, however, for homogeneous ε, the dielectric constant enters the solvation free energy through the expression $(1 - \frac{1}{\varepsilon})$, the relative effect of such an increase will not be quantitatively large (whereas a decrease in ε could be more significant). In an organic biophase though, where ε is smaller, the relative effects of ions could be very significant, but they tend to be excluded from such phases. Even in aqueous solution and even when the relative change in the solvation free energy is small, the absolute effect of ions may be significant, especially for reactions involving ions [124] and electrostatics [125, 126], in both of which cases the magnitude of the total electrostatic free energy is large.

2.2 NON-ELECTROSTATIC CONTRIBUTIONS

It should be clear from the presentation in the previous section that the SCRF method is a model that by design focuses on only one physical effect accompanying the insertion of a solute in a solvent, namely the bulk polarization

of the solvent by the mean field of the solute. Thus the model admittedly neglects all other physical effects. One of these, electron correlation between the solute and the solvent, was mentioned explicitly already. This and other physical effects missing in the SCRF method are discussed in more detail in this section. As a shorthand we call these effects "non-electrostatic" (and abbreviate them *N*), but a more precise wording would be that used in Section 1, namely *and* "non-bulk-type electrostatic."

Electron correlation between the solute and solvent has an important quantitative effect on the solvation free energy. The most important qualitative manifestation of this correlation is the existence of dispersion interactions between solute and solvent (dispersion interactions are neglected in both the Hartree and Hartree-Fock approximations). The solute-solvent dispersion interactions are inseparable in practice from several other effects that are often grouped under the vague heading of cavitation. If we make a cavity in a solvent B to accommodate a solute A, the solvent molecules in the first solvation shell gain A–B dispersion and repulsive interactions, but at the expense of B–B ones. This tradeoff may have significant effects, both enthalpic and entropic, on solvent structural properties. The dispersion and solvent structural aspects of cavitation are two physical effects not accounted for in the treatment of the previous section, with its assumption of an uncorrelated, homogeneous dielectric medium with dielectric constant equal to the bulk value.

Certain aspects of the solvent structural changes in regions near to the solute have received specialized attention and even inspired their own nomenclature. Two examples, each with a long and distinguished theoretical history, are the "hydrophobic effect" and "dielectric saturation."

The hydrophobic effect refers to certain unfavorable components of the solvation free energy when a nonpolar solute is dissolved in water. The most generally accepted explanation (no explanation is universally accepted) starts from the premise that a typical cluster of water molecules in the bulk makes several hydrogen bonds and has several ways to do so. When a non-hydrogen-bonding solute is introduced, the neighboring water molecules will still make about the same average number of hydrogen bonds (although enthalpic components of hydrophobicity, when observed, may sometimes be ascribed to a reduced total number of hydrogen bonds), but they will have less ways to do so since the opportunities for maximum hydrogen bonding will restrict the orientation of solvent molecules in the first solvation shell, and flipping a hydrogen-bonded cluster will not provide the same possibilities for hydrogen bonding as it does in the bulk where the cluster is surrounded on all sides by

water. Thus the water structure in the first hydration shell is more "rigid," which is entropically unfavorable.

Dielectric saturation refers to the breakdown of linear response in the region near the solute. At high enough fields, the permittivity of a dielectric medium is not a constant; it depends on the field [116, 127]. The field in the vicinity of the solute may be high enough that this concern becomes a reality, and the solvent may fail to respond with the same susceptibility as bulk water responds to small applied fields. This will be especially likely to be a problem for multiply charged, small ions [128, 129]. Bucher and Porter [130] have analyzed the dielectric saturation effect quantitatively for ions in water, and they find that the effect of this saturation on the electrostatic contribution to the hydration energy comes primarily from the region within 3 Å of the atomic centers and hence only from the first hydration shell.

Another, related effect leading to non-bulk response in the first hydration shell is electrostriction [131], which is the change in solvent density due to the high electric fields in the first solvation shell of an ion.

A fourth solvent structural effect refers to the average properties of solvent molecules near the solute. These solvent molecules may have different bond lengths, bond angles, dipole moments, and polarizabilities than do bulk solvent molecules. For example, Wahlqvist [132] found a decrease in the magnitude of the dipole moment of water molecules near a hydrophobic wall from 2.8 D (in their model) to 2.55 D, and van Belle et al. [29] found a drop from 2.8 D to 2.6 D for first-hydration-shell water molecules around a methane molecule.

Dispersion is not the only short-range force that needs to be added to the electrostatic interactions. For example, hydrogen bonding is not 100% electrostatic but includes covalent aspects as well, and exchange repulsion is not included in classical electrostatics at all. An accurate model should take account of all the ways in which short-range forces differ from the electrostatic approximation with the bulk value for the dielectric constant.

All these overlapping effects, namely cavitation, solute-solvent dispersion interactions, other solute-solvent electron correlation effects, hydrophobic effects, dielectric saturation, and non-bulk properties of solvating solvent molecules, would be expected to be most significant in the first solvation shell, and numerous molecular dynamics simulations have borne this expectation out [133-137]. One might hope, in light of this, to treat such effects by treating all solvent molecules in the first solvation shell explicitly. In this section, however, we wish to make the point that continuum models need not be abandoned for treating such effects. In fact, continuum models have some significant advantages for such treatments, just as they do for treating bulk electrostatic effects.

The key to the continuum treatment of first solvation-shell effects is the concept of solvent-accessible surface area, introduced by Lee and Richards [63] and Hermann [64]. In a continuum treatment of the solvent, it is useful to define a non-integer "number" of solvent molecules in the first solvation shell so that in some sense this continuous number simulates the average of the integer number of discrete molecules in the first solvation shell in a treatment with explicit solvent molecules. If we imagine a continuous first hydration shell and pass a hypersurface through the middle of the shell, then the simplest assumption is that the average number of solvent molecules in the first solvation shell is proportional to the area of this hypersurface. This area is called the solvent-accessible surface area A. Other possible definitions of molecular surface area do not have this interpretation [138]. Because the surface tensions are empirical they can make up for many flaws in the model. For example, simulations have shown that, due to the dominance of water-water hydrogen bonding, hydrophobic crevices are not accessed by the solvent as much as would be predicted by the calculated solvent-accessible surface areas. Environment-dependent surface tensions can and do make up for such deficiencies in the model in an average way [139].

Since many of the effects that need to be added to the bulk electrostatics are localized in the first solvation shell, and since the solvent-accessible surface area is proportional to the number of solvent molecules in the first solvation shell, it is reasonable to assume that the component of the free energy of solvation, G_N^o, is proportional to the solvent-accessible surface area. A critical refinement of this idea is the recognition that the contribution per solvent molecule of the first-solvation shell in contact with one kind of atom is different from that in contact with another kind of solute atom. If we divide the local surface environment of a solute into several types of region, $\alpha = 1, 2, \ldots$ (e.g., $\alpha = 1$ might denote amine–like nitrogen surface, $\alpha = 2$ might denote nitrile-like nitrogen surfaces, $\alpha = 3$ might denote the surface of carbonyl oxygens, etc.), and if we partition A into parts A_α associated with the various environments of type α, then it is even more reasonable to write

$$G_N^o = \sum_\alpha \sigma_\alpha A_\alpha \tag{53}$$

where each σ_α is some proportionality constant with units of surface tension.

Although entropy cannot be strictly localized, some contributing factors to the solvent entropy change induced by the solute are localized in the first solvent shell, and contributions to the entropy of mixing that are proportional to the number of solvent molecules in the first solvation shell might sometimes

dominate σ_α as well. In assessing such entropic effects there has been considerable attention paid to the effects of size and shape. A nice overview of the current status of our understanding in this area, along with further original contributions, has been provided by Chan and Dill [140]. From a more empirical standpoint, we expect that these size effects, if and when present, may well scale with solvent-accessible surface area [141].

Clearly, since it includes so many effects (see above), σ_α can be positive or negative. Sometimes one effect will dominate, e.g., dispersion or solvent structural change. If the σ_α are determined empirically, they can also make up for fundamental limitations of the bulk electrostatic treatment (such as the intrinsically uncertain location of the solute/bulk boundary and also for systematic errors in the necessarily approximate model used for the solute.

We summarize this section by emphasizing that we have identified a host of effects, and we have seen that they are mainly short-range effects that are primarily associated with the first solvation shell. A reasonable way to model these effects quantitatively is to assume they are proportional to the number of solvent molecules in the first hydration shell with environment-dependent proportionality constants.

Some workers have attempted to treat particular effects more rigorously, e.g., by scaled-particle theory [142] or by extending [95, 103] Linder's theory [143] of dispersion interactions to the case of an SCRF treatment of solute-solvent interactions. We will not review these approaches here.

Finally, we note that we have mostly limited attention so far to the self-consistent reaction field limit of dynamical solvent polarization, which is the only one that has been generally implemented (see next Section). Nevertheless, there are problems where the solute-solvent dynamical correlation must be considered, and we will address that topic in Section 5.

3 Implementations

As reviewed above, when a solute is placed in a dielectric medium, it electrically polarizes that medium. The polarized medium produces a local electrostatic field at the site of the solute, this field polarizes the solute, and the polarized solute interacts with the polarized medium. The interaction is typically too large to be treated by perturbation theory, and some sort of self-consistent treatment of polarized solute and polarized medium is more appropriate. At this point several options present themselves. It promotes orderly discussion to classify these

options, but because there are many aspects, one needs several classification elements. The elements and the popular choices are as follows:

E. How to treat the electrostatics (*E*):
   - E-A. Numerical or analytic solution of the classical electrostatic problem (e.g., Poisson equation) with homogeneous dielectric constant for solvent.
   - E-B. A model solution to the electrostatic problem, e.g., the Generalized Born Approximation or a conductor-like screening solution.
   - E-C. Electrostatics treated empirically, without reference to solute charge distribution.

S. What shape (*S*) to assume for the boundary between the solvent, considered as a continuum, and the solute:
   - S-A. Taking account of molecular shape, e.g., treating the solute as a set of atom-centered spheres.
   - S-B. Treating the solute as an ellipsoid.
   - S-C. Treating the solute as a sphere.

L. At what level (*L*) to model the solute:
   - L-A. With polarizable charges obtained by an approximate quantum mechanical method including electron correlation or by a Class IV charge model.
   - L-B. With polarizable charges obtained by the *ab initio* Hartree-Fock method.
   - L-C. With polarizable charges obtained by semiempirical molecular orbital theory.
   - L-D. With polarizable charges obtained by A, B, or C combined with a truncated multipole expansion, including multipole moments up to some predetermined cutoff l, where $l > 1$ but not necessarily large enough for convergence.
   - L-E. Like D but with only $l = 0$ and/or 1.
   - L-F. By non-polarizable charges, e.g., as might be used in a molecular mechanics calculation, or an unpolarized charge

density on a grid. (Use of non-polarizable dipole moments, i.e., permanent rather than permanent plus induced, would also fit in here.)

N. Whether to augment the electrostatics terms by an estimate of non-electrostatic (*N*) contributions:
   - N-A. Yes, including empirical elements to make up for the approximate character of the electrostatics as well as to include other identifiable effects.
   - N-B. Yes, treating one or more non-electrostatic interactions non-empirically.
   - N-C. Yes, by a single linear function of molecular surface area.
   - N-D. No.

Although the list of choices is lengthy, we should also note some choices that are *not* present. With regard to the electrostatic (*E*) element, all models currently in general use assume a homogeneous dielectric constant for the solvent, thereby neglecting possible dielectric saturation in the first solvation shell and also neglecting the fact that solvent molecules near to the solute have different properties (average dipole moment, polarizability, geometry, size, and hence dielectric constant) than bulk solvent molecules. (Note, though, that Hoshi [144] and Tomasi and co-workers [145-148] have discussed algorithmic implementations of an inhomogeneous dielectric continuum in SCRF models, and note also that both dielectric saturation and the unique properties of the solvent molecules in the first solvation shell *are* included in models that make choice A for element *N*.) With regard to the shape (*S*) element, all choices assume a well defined discontinuous change of dielectric properties at a fixed, sharp solute/solvent boundary. In reality of course, this boundary is a fluctuating, finite-width boundary *layer*. With regard to the level (*L*) element, we note that the ideal choice of "by converged quantum mechanics" is missing, for reasons of practicality. The missing choices have an important consequence for which combinations of the other choices seem most suitable. For example, one asks, given that the assumption of homogeneous dielectric constant, the assumption of a rigid, sharp solute/solvent boundary, the assumption of an approximate solute wave function, and the neglect of solute-solvent exchange repulsion all introduce significant approximations into the electrostatics, is it still worthwhile to solve the Poisson equation numerically, or would an approximate solution introduce errors smaller than those already inevitably present? Different workers have answered

such questions differently. We believe, in fact, that more than one answer to such questions is justifiable, and there is room in the computational toolbox for more than one tool, with the best choice depending on the application.

Tables 1 and 2 provide a list of recently proposed solvation models and classifies them according to the above scheme. For convenience, each row of the table is given a label. In some cases the label is based on a well established name or acronym (e.g., PCM, SM*x*), or an acronym to be used in this chapter. The acronyms to be used in labels are as follows:

SCME	single-center multipole expansion
DO	dipole only (SCME with $l \leq 1$)
DME	distributed multipole expansion
PCM	polarized continuum model
PE	Poisson equation (direct solution in physical space)
GB	generalized Born (approximation)
COSMO	conductor-like screening model
GCOSMO	generalized COSMO
/ST or /SA	plus surface tensions
SASA	solvent-accessible surface area
TBS	truncated basis set
SM*x*	Solvation model *x* (a name we give to our own parameterized GB/ST models)
AM1aq	Austin model 1 aqueous

In other cases we base the label on the author's initials. Next we comment on the methods in the tables and some aspects of the issues they raise.

The oldest methods are based on multipole expansions. Because these methods have been around for a long time, and because they lend themselves to appealing analytical solutions if further approximations are made, they have developed a history of sometimes being used with additional, unrealistic assumptions. The two most important of these further assumptions are truncating the multipole expansion at the dipole term (DO) and replacing the solute cavity by a sphere or ellipsoid. We now recognize, though, that these further approximations are usually unwarranted; indeed, we recommend that methods employing either or both of these approximations should be avoided for serious work.

TABLE I
Continuum models based on electrostatics only.

Label	Authors	Reference(s)	Elements			
			E	*S*	*L*	*N*
Models with *S* = B, C, and/or *L* = D, F						
PE1	Honig group	[149-151]	A	A	F	D
PE2	Rashin	[152]	A	A	F	D
PE3	McCammon group	[153]	A	A	F	D
PE4	Lim, Chan, Tole	[154]	A	A	F	D
DO	Kirkwood, Onsager	[61, 155]	A	C	F	D
DO1	Tapia, Goscinski	[91]	A	C	E	D
DO2	Szafran, Karelson, Katritzky, Zerner	[156, 157]	A	C	E	D
DO3	Wong, Wiberg, Frisch	[99, 158]	A	C	E	D
DO4	Freitas, Longo, Simas	[159]	A	C	E	D
DO5	Adamo, Lelj	[160]	A	C	E	D
GB1	Tucker, Truhlar	[161]	B	A	F	D
SCME	Kirkwood, Onsager	[61, 155]	A	C	F	D
SCME1	Rivail, Rinaldi	[88]	A	C	D	D
SCME2	Rivail, Terryn	[162, 163]	A	B	D	D
SCME3	Chipot, Rinaldi, Rivail	[100]	A	B	D	D
SCME4	Dillet, Rinald, Rivail	[164, 165]	A	A	D	D
SCME5	Mikkelsen et al.	[93, 106]	A	C	D	D
SCME6	Ford, Wang	[166]	A	B	D	D
SCME7	Pappalardo, Reguero, Robb, Frisch	[167]	A	B	D	D
DME	Huron, Claverie	[168]	A	C	F	D
DME1	Friedman	[169]	A	C	D	D
DME2	Gersten, Sapse	[170]	A	B	F	D
DME3	Karlström	[171]	A	C	B	D
DME4	Karelson, Tamm, Zerner	[172]	A	C	C	D
TBS	Kim, Bianco, Gertner, Hynes	[173, 174]	B	C	F	D

TABLE I (continued)
Continuum models based on electrostatics only.

Label	Authors	Reference(s)	Elements *E*	*S*	*L*	*N*
Models with untruncated, polarizable charge distributions and shape sensitivity						
PCM	Miertus, Scrocco, Tomasi	[175]	A	A	B	D
PCM2	Hoshi et al.	[144, 176, 177]	A	A	C	D
PCM3	Ford and Wang	[178, 179]	A	A	C	D
PCM4	Fox, Rösch, Zauhar	[180, 181]	A	A	C	D
PCM5	Negre, Orozco, Luque	[182, 183]	A	A	C	D
PCM6	Rashin, Bukatin, Andzelm, Hagler	[184]	A	A	A	D
PE4	Baldridge, Fine, Hagler	[185]	A	A	A	D
PE5	Chen, Noodleman, Case, Bashford	[186]	A	A	A	D
GB2	Peradejordi	[187]	B	A	C	D
GB3	Kozaki, Morihasi, Kikuchi	[188, 189]	B	A	C	D
DME5	Tapia, Colonna, Angyan	[112]	A	A	B	D
DME6	Dillet, Rinaldi, Ángyán, Rivail	[164]	A	A	A	D
COSMO	Klamt, Schüürmann	[190]	B	A	C	D

TABLE II
Classification of continuum models that include both electrostatic and non-electrostatic contributions.

Label	Authors	Reference(s)	Elements *E*	*S*	*L*	*N*
Models with $S \leq$ B, C and/or L = D, F						
SASA	Hermann	[64]	C	A	F	A
SASA1	Eisenberg	[191]	C	A	F	A
SASA2	Ooi, Oobatake, Némethy, Scheraga	[192]	C	A	F	A
GB/SA	Still et al.	[193]	B	A	F	C
SCME/RCR	Rinaldi, Costa Cabral, Rivail	[194]	A	B	D	B
SCME/RRR	Rivail, Rinaldi, and Ruiz-López	[95]	A	A	D	B
SCME/YGHB	Young, Green, Hillier, Burton	[195]	A	B	D	A
SCME/TSB	Tuñón, Silla, Bertrán	[196]	A	B	D	A
DME/ST/LCCP	Langlet, Claverie, Caillet, Pullman	[197]	A	A	D	B
DME/ST/SK	Sato, Kato	[198]	A	C	B	B
PCM7	Purisima and Nilar	[199]	A	A	F	C
PCM8	Varnek et al.	[200]	A	A	F	A
KH	Karlström and Halle	[201]	B	C	D	B
BCN	Basilevsky, Chudinov, Newton	[110]	B	C	C	B
Models with untruncated, polarizable charge distributions and shape sensitivity						
PCM/ST/FTP	Floris, Tomasi, and Pascual-Ahuir	[202, 203]	A	A	B	B
PCM/ST/OAT	Olivares del Valle, Aguilar, Tomasi	[97, 103, 104]	A	A	A	B
PCM/ST/YGHB	Young, Green, Hillier, Burton	[195]	A	A	B	B
PCM/ST/A	Amovilli	[204]	A	A	B	B
PCM9/ST	Bachs, Luque, and Orozco	[205]	A	A	B	A
PCM10/ST	Orozco, Luque, coworkers	[205-209]	A	A	C	A
GB/ST/SM1-3.1	Cramer and Truhlar	[210-215]	B	A	C	A
GB/ST/SM4&5	Cramer and Truhlar	[213, 216-218]	B	A	A	A
PCM/D	Rauhut, Clark, Steinke	[219]	A	A	C	B
PE/ST/FGH	Friesner, Goddard, Honig	[220]	A	A	A	C
AM1aq	Dixon, Leonard, Hehre	[221]	B	A	C	A
GCOSMO	Truong and Stefanovich	[222, 223]	B	A	A	C

If the cavity is not simplified and terms are added to the multipole expansion until it converges, the result is exact and none of the unphysical consequences of a truncated multipole expansion remain. One difficulty with this approach though is that the multipole series is not necessarily convergent at small distances. A second is that for large molecules, a single-center expansion is a very unnatural way to represent the electrostatics. Even very small molecules may require large numbers of terms in the multipole expansion to converge it. For example, a treatment of electron scattering by acetylene that employed a single-center multipole expansion contained terms with l up to 44 in an attempt to converge the anisotropy of the electrostatics [224].

One way around the slow convergence of single-center expansions is a multi-center multipole expansion [225-229]. Several workers have explored the utility of DME within the SCRF framework [112, 164, 171]. Of course, when the multipoles do not reside at atomic positions, it is clear that calculation of such quantities as analytic energy derivatives will become more difficult.

Alternatively one can avoid multipole expansions altogether. There are two main approaches in use for solving the electrostatic problem without a multipole expansion. One of these solves the Poisson equation in terms of virtual charges on the surface of the primary subsystem. This is usually called the polarized continuum model (PCM) in quantum chemistry although it is called a boundary element method in the numerical analysis literature. The second approach solves the Poisson equation directly in the volume of the solvent, e.g., by finite differences. The latter approach will be called a Poisson equation (PE) approach. We should keep in mind, however, that SCME, DME, PCM, and PE methods will all lead to (the same) accurate electrostatics if the numerical methods are taken to convergence and there is no difference due to the handling of other "details.". One such detail that might be mentioned is charge penetration outside the cavity. By construction in the PCM model, the small amount of electronic density outside the cavity is eliminated from the surface charge computations and as a result the solute bears a very small charge. Tomasi has emphasized the need to correct for this phenomenon [79], but his approach has yet to be adopted by other groups doing PCM calculations.

As mentioned above, the PCM is based on representing the electric polarization of the dielectric medium surrounding the solute by a polarization charge density at the solute/solvent boundary. This solvent polarization charge polarizes the solute, and the solute and solvent polarizations are obtained self-consistently by numerical solution of the Poisson equation with boundary conditions on the solute-solvent interface. The free energy of solvation is obtained from the interaction between the polarized solute charge distribution and the self-

consistent surface charge distribution [175]. The physics is the same for the PCM and PE approaches (and for the fully converged SCME or DME, for that matter), although the numerical methods are different.

The next question to be discussed was already mentioned in Section 2.1, namely, since the electrostatic problem, with its sharp boundary and its homogeneous solvent dielectric constant, already represents a somewhat unrealistic idealization of the true molecular situation, how important is it to solve that problem by exact electrostatics? We would answer that this is not essential. Although it presumably can't hurt to solve the electrostatics accurately, except perhaps by raising the computer time, it may be unnecessary to do so in order to represent the most essential physics, and a simpler model may be more manageable, more numerically stable, and even more interpretable. This is the motivation for the GB approximation and COSMO.

GB-like approximations [41, 71, 119, 161, 187, 189, 230-233] may be derived from eq (1) by using the concept of dielectric energy density, as in the work of Bucher and Porter [130], Ehrenson [131], and Schaefer and Froemmel [234]. As the GB methodology has been extensively reviewed in the recent past [81, 83, 213], we confine our presentation to a very brief discussion of the key aspects of the theory. The polarization free energy in the GB model is defined as

$$G_P(aq) = -\frac{1}{2}\left(1-\frac{1}{\varepsilon}\right)\sum_{k,k'} q_k q_{k'} \gamma_{kk'}, \tag{54}$$

where ε is the solvent dielectric constant, q is the net atomic charge, k labels an atomic center, and $\gamma_{kk'}$ is a coulomb integral, which in atomic units is the reciprocal of an effective radius (monatomic diagonal terms) or effective distance (diatomic off-diagonal terms). The descreening of individual parts of the solute from the dielectric by other parts of the solute is accounted for in these effective quantities. In particular, in our work we use an empirical functional form for γ that was proposed by Still et al. for their GB/SA model [193]. The present authors modified that form in several ways, including making it a function of atomic partial charges, in the development of the SM1 [210], SM1a [210], SM2 [211], SM2.1 [214], SM2.2 [215], SM3 [212], SM3.1 [214], and SM4 [213, 216, 217] GB/ST solvation models. The SM5 solvation model [218] further modifies γ so that it may be expressed purely as a function of geometry, i.e., it has no explicit dependence on elements of the density matrix, thereby facilitating the calculation of analytic energy derivatives. The SM4 and SM5 solvation models are based on Class IV charge models [235], which provide the best available estimates of partial charges for electrostatics calculations.

The E, N, and P terms are then obtained from the density matrix **P** of the aqueous-phase SCF calculation as

$$G_{ENP} = \frac{1}{2}\sum_{\mu\nu} P_{\mu\nu}\left(H_{\mu\nu} + F_{\mu\nu}\right) + \frac{1}{2}\sum_{k,k'\neq k} \frac{Z_k Z_{k'}}{r_{kk'}} \qquad (55)$$

where **H** and **F** are respectively the one-electron and Fock matrices, μ and ν run over valence atomic orbitals, and Z_k is the valence nuclear charge of atom **k** (equal to the nuclear change minus the number of core electrons). When the net atomic charge q in equation 54 is determined by Mulliken analysis of the NDDO wave function, the Fock matrix is simply given by [71, 210, 236]

$$F_{\mu\nu} = F^{(0)}_{\mu\nu} + \delta_{\mu\nu}\left(1-\frac{1}{\varepsilon}\right)\sum_{k',\mu'\in k'}\left(Z_{k'} - P_{\mu'\mu'}\right)\gamma_{kk'}, \quad \mu\in k \qquad (56)$$

where $\delta_{\mu\nu}$ is the Kronecker delta function. This approach was used in the SM1, SM1a, SM2, and SM3 solvation models. The SM4 alkane models [216, 217] an interim SM4 water model specific for selected kinds of {C,H,O} compounds [213], and SM5 models, on the other hand, use Class IV Charge Model 1 (CM1) partial atomic charges [213, 235], which provide a more accurate representation of the electronic structure. This renders eq 56 somewhat more complex [216], but does not change its basic form. In all SM*x* models, the density matrix is determined self-consistently in the presence of solvent.

Values of G_{ENP} calculated from the GB approximation compare well to values obtained from numerical solution of the Poisson equation for similar collections of point charges [83, 237, 238]. A very promising extension of the GB methods is provided by a new scaled pairwise approximation to the dielectric screening integrals [215].

The COSMO method is a solution of the Poisson equation designed primarily for the case of very high ε [190]. It takes advantage of an analytic solution for the case of a conductor ($\varepsilon = \infty$). The difference between $(1 - \frac{1}{\varepsilon})$ for the case of $\varepsilon = 80$ and $\varepsilon = \infty$ is only 1.3%, so this is a good approximation for water. Its use for the treatment of nonpolar solvents with $\varepsilon \approx 2$ depends on further approximations which have not yet been sufficiently tested to permit an evaluation of their efficacy.

Finally we address the issue of contributions. In our view it is unbalanced to concentrate on a converged treatment of electrostatics but to ignore other effects. As discussed in section 2.2, first-solvation-shell effects may be included in continuum models in terms of surface tensions. An alternative way to try to include some of them is by scaled particle theory and/or by some *ab initio* theory

of dispersion. Table 2 summarizes continuum models that attempt to treat both electrostatic and first-solvation-shell effects.

Some models carry the surface tension approach to extreme, and attempt to include even the electrostatic contributions in the surface tensions. These pure SASA models are obviously limited in their ability to account for such phenomenon as dielectric screening, but they have the virtue of being very easy to compute. Thus, they can be used to augment molecular mechanics calculations on very large molecules with a qualitative accounting for solvation.

Also within the molecular mechanics framework is the molecular-mechanics-type GB/SA model of Still et al. [193] In this instance, the electrostatics are handled by a Generalized Born model, but the atomic charges are parametric. They are chosen in such a way that Still et al. assign only a single surface tension to the entire molecular solvent-accessible surface area; this is also done in the PE/ST/FGH and PCM10 models. All these authors rationalize this by calling the ST part a hydrophobic term, but it is clear that other non-electrostatic effects must then be being absorbed into the cavity parameterization and, in Still et al.'s MM case, possibly into the partial atomic charges.

Many groups have chosen to specifically calculate cavitation and/or dispersion terms. The former typically are computed by the scaled particle theory, following Pierotti [142], while several different approaches have been formulated for the latter. Ultimately, however, there are non-electrostatic components of the solvation free energy remaining that do not lend themselves to ready analysis. Bearing that in mind, it is not clear that there is much point in spending resources calculating any one non-electrostatic component more rigorously than the others. Thus, the most general approach is to parameterize *all* non-electrostatic effects into atomic surface tensions (so as to reproduce experimental free energies of solvation after the electrostatic components have been removed). This is the philosophy guiding the SM*x*, AM1aq, PCM9/ST, PCM10/ST, and SCME/TSB models, and an increasing number of workers appear to be moving in this direction.

4 Solvation effects on equilibrium properties

As discussed in Section 2, one key assumption of reaction field models is that the polarization field of the solvent is fully equilibrated with the solute. Such a situation is most likely to occur when the solute is a long-lived, stable molecular structure, e.g., the electronic ground state for some local minimum on a Born-Oppenheimer potential energy surface. As a result, continuum solvation models

based on reaction fields should be especially useful for the prediction of solvent effects on equilibrium constants.

Equilibria may take a number of forms—constitutional, tautomeric, conformational, etc. For any equilibrium problem in solution, one may consider the free energy cycle depicted in the figure below, where A and B label different molecules or different isomers of the same molecule, depending on the type of equilibrium. The scheme below shows that the free energy change for a reaction or tautomerization on going from the gas phase into solution is equal to the difference in the free energies of solvation of the initial and final species (the figure depicts a unimolecular reaction, but this statement is true in the general case).

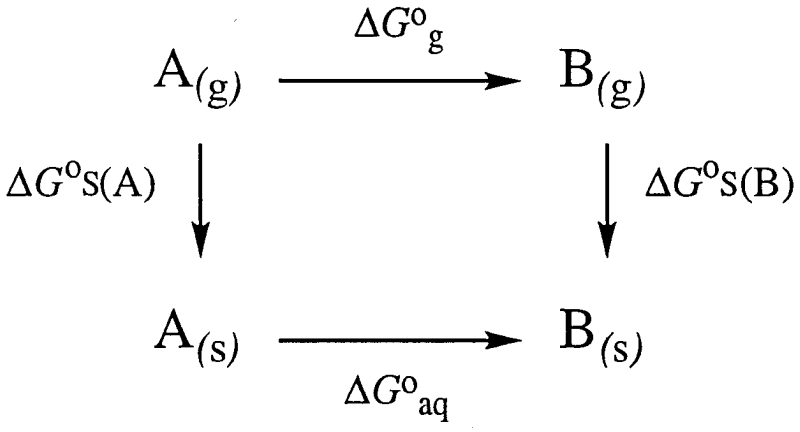

$$\Delta G^{o}_{aq} = \Delta G^{o}_{g} + \Delta G^{o}S(B) - \Delta G^{o}S(A)$$

Tautomeric equilibria involving populations of isomers that differ by bond connectivity are of special interest for the study of solvent effects, and such equilibria involving heterocycles have proven to be a favorite testing ground for developers of continuum solvation models. For protomeric heterocyclic equilibria, this is at least partly due to the very large changes in one-electron properties (e.g., the dipole moment) that affect the solvation free energy when the proton substitution pattern changes.

In this section we will consider only equilibria in which the number of moles of solute does not change. In such cases the population of a given contributor to the equilibrium may be calculated by using a standard Boltzmann formalism, i.e., the fraction of species A is

$$F(\mathrm{A}) = \frac{e^{-G^{\circ}_{\mathrm{A}}/RT}}{\sum_{\mathrm{B}} e^{-G^{\circ}_{\mathrm{B}}/RT}} \tag{57}$$

where G may be either a gas phase or a solution value, and the sum over B runs over all equilibrium contributors. In below discussion we will take %(A) ≡ 100 F(A). When free energies in both the gas phase and in solution are available, one may calculate [239] the absolute free energy of solvation, $\Delta G^{\circ}_{\mathrm{S}}$, as

$$\Delta G^{\circ}_{\mathrm{S}} = -RT \ln\left\{\sum_{\mathrm{A}}\left[\frac{\mathrm{e}^{-G^{\circ}_{gas}(\mathrm{A})/RT}}{\sum_{\mathrm{B}} \mathrm{e}^{-G^{\circ}_{gas}(\mathrm{B})/RT}}\right] e^{-\Delta G^{\circ}_{\mathrm{S}}(\mathrm{A})/RT}\right\} \tag{58}$$

where the sums over both B and A run over all contributors.

This section will focus on the application of dielectric continuum models to equilibria like those described above. A special effort will be made to highlight investigations that compared two or more solvation models. We emphasize that some care must be taken to distinguish the degree to which different continuum models have been extended to account for non-electrostatic effects, since these effects may certainly play a large role in some of the equilibria under discussion. Those continuum models that consider only electrostatics are of limited applicability unless non-electrostatic effects cancel for all equilibrium contributors.

We will begin with a discussion of reaction equilibria, including acid-base reactions and more complex bond-making/bond-breaking reactions. We will then move on to tautomeric equilibria. We note that Reichardt [240] has provided a thorough compilation of many equilibria, including most of those discussed below, where solvent effects had been studied experimentally and/or using some theoretical model, as of 1990. On the theoretical side, at least, the number of systems studied has greatly expanded since then.. Whereas Reichardt summarizes the use of linear free energy relationships for predicting such equilibria, a large amount of the recent work is based on SCRF models.

4.1 REACTION EQUILIBRIA

As one might expect, reactions that create, destroy, or separate charge tend to exhibit very large solvation effects. The most common examples of such reactions

are Brønsted acid-base equilibria. A particularly striking example is available for the special case of an *internal* acid-base proton transfer, which is also a special case of a tautomeric equilibrium. This occurs, for example, when amino acids are placed in water. Several continuum modeling studies have focused on this equilibrium for glycine, and they are summarized in section 4.1.1. Intermolecular proton transfers have also been the subject of several studies, particularly transfers between amine bases; these investigations are described in section 4.1.2.

4.1.1 Intramolecular proton transfer

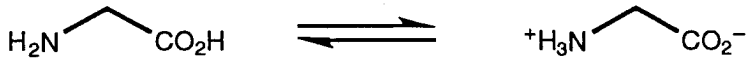

1 **2**

At biological pH, glycine exists exclusively in its zwitterionic form **2** [241], whereas in the gas phase, only the non-zwitterionic species **1** is observed [242]. In the absence of solvation, the zwitterion is not a stationary point, but instead undergoes spontaneous proton transfer back to the neutral form. In an early study, Bonaccorsi et al. [243], using the PCM model, showed that a continuum solvation model can account for the stability of the zwitterion in aqueous solution. Although they made some comparison to the experimental enthalpy for the transfer of **1** from the gas phase to **2** in aqueous solution (-19.2 ± 1 kcal/mol) [244], this particular study emphasized the sensitivity of the computational results to solute geometries (many of those discussed were unoptimized), basis set, and cavity size. Thus, the calculated gas-phase proton transfer energy ranges from 20 to 40 kcal/mol at the HF/4-31G [245] level, to 65 to 90 kcal/mol at the HF/STO-3G level. Different prescriptions for choosing the zwitterion cavity yielded solvation free energies varying from –36.2 kcal/mol to –57.3 kcal/mol. Since the zwitterion is not stationary in the gas phase, the experimental enthalpy of transfer cited above cannot be separated into proton transfer and solvation components (and the entropic aspects are similarly unclear, making comparison to reaction field free energies results difficult). Hehre et al. [246] used the AM1-SM2 model to study the solvation of neutral and zwitterionic glycine, and found the zwitterionic form to be better solvated by 25 kcal/mol in aqueous solution. Adding this differential free energy of solvation to the relative gas phase free energy difference (using a frozen zwitterion geometry) of 17.8 kcal/mol favoring the neutral form at the HF/3-21+G level, they predict the zwitterion to be the preferred form in aqueous solution by 7.6 kcal/mol.

4.1.2 Intermolecular proton transfer

In the gas phase, simple deprotonations tend to be barrierless reactions leading to a high-energy separated proton and anion, but solvation can change the situation even qualitatively. Pietro has emphasized the pedagogical utility of employing a continuum solvation model (in this case the SM1 model) in a computational study on the deprotonation of nitromethane [247]. When reaction field calculations are used to calculate standard state free energies of conjugate acids and bases in solution, this permits direct calculation of the acid dissociation constant (pK_a). Such calculations of the absolute pK_a are notoriously difficult, since very high levels of theory are required to accurately calculate the gas-phase component of proton affinities and since solvation energies of ions are very large, so that even relative errors in solvation energies can be large on an absolute scale. As a result, most methods for predicting pK_a values tend to be empirical in nature [248-250]. A simpler alternative to calculations of absolute pK_a's is to examine trends in pK_a values for related molecules. In this vein, Rajasekaran et al. [251] have used the finite difference Poisson-Boltzmann method to examine differences in pK_a values for aliphatic dicarboxylic acids. They identify the importance of solvent screening of charge-charge interactions internal to the solute. Urban et al. [252] have employed a similar approach in examining the relative pK_a values for phenol and *ortho-*, *meta-*, and *para*-fluorophenol, using the SM2 and SM3 quantum mechanical solvation models, and the physically similar molecular mechanics GB/SA model. They noted in particular the importance of accounting for non-electrostatic hydrophobic interactions of the fluorine atom. The QM models agree with experiment to within about 1 kcal/mol for the effect of solvation on the relative pK_a values. The MM model does similarly well when charges derived from fitting to the molecular electrostatic potential (ESP) are employed.

Other workers have considered proton transfer reactions between different bases and the effect of solvation on these processes. Terryn and Rivail [253], Galera et al. [254], Pascual-Ahuir et al. [255], Tuñón et al. [256], and Young et al. [195] have all focused on the interesting aqueous basicity trend of the series ammonia, methylamine, dimethylamine, and trimethylamine. In the gas phase, it is well established that the order of basicity for these amines is $Me_3N > Me_2NH > MeNH_2 > NH_3$ [257, 258]. This may be understood on the basis of simple polarizability arguments. However, in aqueous solution, the basicity ordering changes to $MeNH_2 \approx Me_2NH > Me_3N \approx NH_3$ [259]. All of these studies indicate that changes in basicity are dominated by the electrostatic component of the free energy of solvation of the relevant ammonium ions. In aqueous solution, the smaller ions are better solvated, and as a result have lower free energies. These

studies also emphasize, however, how sensitive the results are to choices of basis set and cavity size. In particular, Young et al. [195] compared an ellipsoidal cavity SCRF model with multipole expansions of $l = 1$ and $l = 6$ to the generalized-cavity PCM approach. The ellipsoidal cavity model predicts considerably larger differential solvation free energies between different members of the homologous amine series than does the PCM model, but these differences tend to cancel so that both PCM and the $l = 6$ expansion gave qualitatively correct answers (i.e., proper sign and within about 1 pK_a unit for ΔpK_a on going from the gas phase to aqueous solution). The $l = 1$ expansion, i.e., an ellipsoidal Kirkwood-Onsager model, was less satisfactory, and did particularly poorly when comparing ammonia and methylamine.

The present authors, using the SM*x* series of models, have considered aqueous solvation effects on proton transfer for these same amines, together with several other bases, and have arrived at similar conclusions to those detailed above [83, 236, 260].

Tuñón et al. have considered the inversion of the alcohol acidity scale on passing from the gas phase to solution [261]. They used gas-phase geometries, the PCM method for electrostatics (with a radius for O of 1.68 Å in the alcohol and 1.4 Å in the conjugate base), and separate estimates of dispersion and cavitation energies. They found that increasing the size of the alkyl group decreases the solvation energy of the conjugate base in solution and concluded that this is the primary source of the acidity order.

Finally, studies of proton transfer reactions in aqueous solution where an individual water molecule plays a role that distinguishes it from the bulk solvent have also recently appeared. Rivail et al. [105, 262] have examined the water-assisted ionization of HF and HCl in both nonpolar and polar solutions. Using a generalized multipole reaction field method (with multipoles up to $l = 6$) within an ellipsoidal cavity (to facilitate geometry optimization), they concluded that ionization of HCl requires the specific assistance of two water molecules, and that the resultant cation is better described as $H_5O_2^+$ than as $(H_3O^+)\cdot H_2O$. They also concluded that ionization of HF does not proceed in a polar continuum even with two explicit water molecules included in the cavity. This may be compared to a study by Ando and Hynes [263] in which the bulk water solvent is treated not within the framework of a reaction field formalism, but instead is represented as a generalized solvent coordinate [264]. The energetics associated with the solvent coordinate were determined from Monte Carlo simulations using explicit water molecules for various points along an assumed proton transfer reaction path. Ando and Hynes also included two explicit water molecules in their quantum mechanical treatment. Their key conclusions were that two proton transfer steps

occur adiabatically; the first has a negligible free energy barrier and proceeds with significant motion along the solvent coordinate (i.e., solvent structural rearrangement is required), while the second free energy barrier is about 0.9 kcal/mol and arises primarily from the requirement for nuclear reorganization of the two water molecules. The free energy change associated with this ionization was calculated to be –6.9 kcal/mol (an estimate of –7.5 kcal/mol was offered that includes complete separation of the ions), which may be compared with the experimental ionization free energy of –8 to –10 kcal/mol [265]. Ando and Hynes' findings agree with those of Rivail et al. in that the transferred proton is associated about equally strongly with both of the explicit water molecules; however Ando and Hynes observe this to be the case only after inclusion of zero point vibrational energy, while Rivail et al. find only a single equilibrium structure in the appropriate region of the $(Cl^-)\bullet H_5O_2^+$ potential energy surface.

4.2 TAUTOMERIC EQUILIBRIA

A tautomeric equilibrium is a unimolecular equilibrium in which the various contributors differ based upon bond connectivity. In the special case of a protomeric tautomeric equilibrium, they differ only in how many protons are attached to each heavy atom. In-text figures throughout this section illustrate molecules for which multiple tautomers exist. When the molecules of interest are heterocycles, different tautomers may exhibit very large differences in electronic properties [266]. In particular, they may span a wide range of polarities. That being the case, tautomeric equilibria can be quite sensitive to solvation effects, and they have thus proven to be attractive testing grounds for continuum solvation models.

In a recent review [83], the present authors discussed the tautomeric equilibria of 2-hydroxypyridine/2-pyridone and the 5-(2*H*)-isoxazolone system in considerable detail, focusing on the application of several different continuum solvation models. The following presentation will be somewhat more broad in terms of the different equilibria discussed and will not recapitulate all of the analysis previously presented for the above two systems.

Section 4.2.1 will be devoted to heterocycles, section 4.2.2 will cover other kinds of protomeric tautomeric equilibria (e.g., enol/ketone, formic acid, formamidine, etc.), and section 4.2.3 will discuss an example of a ring/chain tautomeric equilibrium. The order of presentation will be approximately by increasing molecular weight within each section. A review by Kwiatkowski et al. [267] covers work on formamide, pyridines, pyrimidines, purines, and nucleic

acid bases up to 1984, so for these systems our focus will predominantly be on more recent investigations.

We note one general point prior to addressing individual systems. Computational studies aimed at providing quantitative predictions of equilibrium populations in solution *must accurately predict total free energies in solution.* In particular, if the theory employed involves calculating solvation free energies to be added to a gas-phase potential energy surface with thermal rovibrational effects included (and essentially all calculations in solution may be viewed as conforming to this separation of components), then either the gas-phase free energies and the free energies of solvation must both be calculated accurately, or errors in one part of the calculation must be offset by errors in the other. Clearly, the former situation is the more desirable. Where possible, we will provide some analysis of the quality of the gas-phase portions of the following calculations as well. Naturally, when the point of the calculation is merely to provide qualitative indications of relative free energies of solvation for different tautomers, requirements on the accuracy of the levels of theory are less stringent.

4.2.1 Heterocycles

This section is divided into eight subsections, covering imidazoles, pyrazoles, isoxazoles, oxazoles, triazoles, tetrazoles, pyridines, and pyrimidines, purines, and nucleic acid bases respectively.

4.2.1.1 Imidazoles

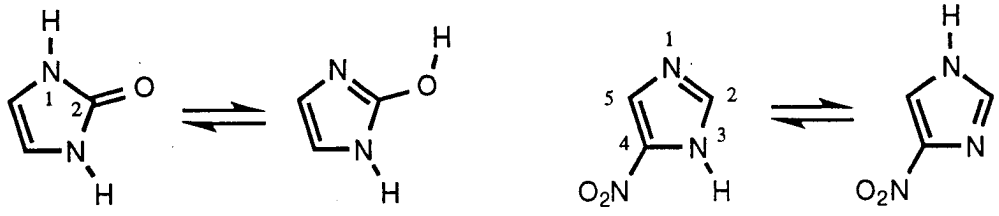

3 **4** **5** **6**

Two tautomeric equilibria have been considered for substituted imidazoles, that between 2-imidazolone **3** and its 2-hydroxyimidazole tautomer **4** [268] and also that between the 1*H* and 3*H* tautomers of 4-nitroimidazole, **6** and **5**, respectively [269, 270]. Karelson et al. used the DO2* model with a spherical cavity of 2.5 Å radius and found 2-imidazolone to be better solvated than its tautomer by 7.7 kcal/mol at the AM1 level. [The asterisk in DO2* indicates that the reaction field

was derived from solution of an incorrect non-linear Schrödinger equation, i.e., not eq 30 [157]. In the DO2* model, a factor of 0.5 precedes the operator K_{op} in eq 30; the result is reduced polarization of the wave function in response to solvation.] AM1 further predicts the gas phase energy difference to favor the oxo tautomer by about 8 kcal/mol. The observed tautomer in solution is the oxo tautomer [266].

Using the same theoretical model, Karelson et al. [269] and later Rzepa et al. [270] examined 4-nitroimidazole. The latter work corrected incomplete geometry optimizations present in the former study. In this instance, AM1 predicts **5** to be 1.4 kcal/mol lower in relative energy than **6**. However, the DO2* model predicts the aqueous solvation free energies to be –25.3 and –7.1 kcal/mol for **6** and **5**, respectively, rendering **6** considerably lower in energy than **5** in solution, which agrees with the experimental situation.

It is clear in both of these studies that the small cavity size (which fails to entirely contain all of the atoms given standard van der Waals radii) causes electrostatic solvation free energies to be seriously overestimated—the difference in the 4-nitroimidazole system seems much too large to be physically reasonable. This overestimation would be still *more* severe were a correct DO model to have been used (i.e., one which accounted self-consistently for the full solute polarization using eq 30). Nevertheless, the DO2* results may be considered qualitatively useful, to the extent that they identify trends in tautomer electrostatic solvation free energies.

One measure of the inaccuracy associated with the small cavity radius may be had from the calculations of Orozco et al. [207], who also studied the 4-nitroimidazole system using the PCM8/ST model. The general cavity in this case was constructed from atom-centered spheres having typical van der Waals radii [207]. At the AM1 level, the differential electrostatic free energy of hydration is predicted to be only 4.5 kcal/mol; this may be compared to the value of 18.2 kcal/mol noted above for the DO2* model. Orozco et al. [207] also included first-solvation-shell effects, which they found to favor **5** by 1.2 kcal/mol, leading to a net differential free energy in solution (AM1 + PCM8/ST) of 2.1 kcal/mol.

4.2.1.2 Pyrazoles

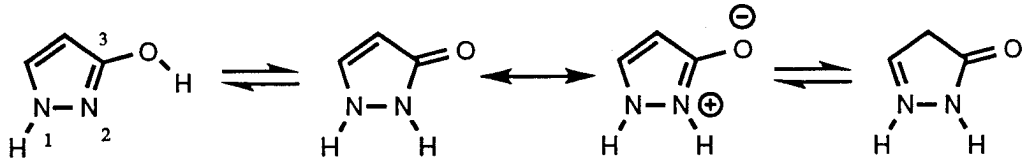

7 **8a** **8b** **9**

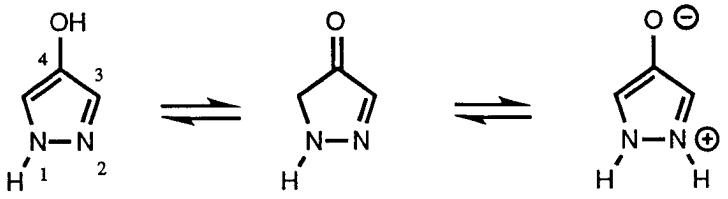

10 **11** **12**

Karelson et al. [268] also used the AM1 DO2* method with a spherical cavity of 2.5 Å radius to study tautomeric equilibria in the 3- and 4-hydroxypyrazole systems, **7-9** and **10-12**, respectively. Rzepa et al. [270] later corrected the results for incomplete geometry optimization in the latter heterocycle. Although the observed [266] forms in aqueous solution are the oxo tautomer **8** (i.e., the pyrazolone) in the first case and the zwitterion **12** in the latter case, gas-phase AM1 calculations predict these tautomers to be much higher in relative energy than the corresponding hydroxy tautomers **7** and **10**, respectively. In each case, it was found that the DO2* method successfully predicted the observed aqueous tautomer. However, the DO2* electrostatic solvation free energy for **12** was predicted to be –57.3 kcal/mol! As for the nitroimidazole results discussed in the last section, this number is incredibly large, probably as a result of the small cavity radius chosen. However, so large a solvation free energy was required in order to overcome a very unfavorable gas-phase energy predicted by AM1 (about 40 kcal/mol higher than the other two tautomers). It seems likely that the AM1 relative energy is inaccurate, given the experimental situation and the very small likelihood of two tautomers differing in solvation free energy by so large an amount.

One qualitative result of particular interest arises in the study of 3-hydroxypyrazole. The electronic structure of the oxo tautomer **8** may be thought of as having two mesomeric (i.e., resonance) contributors **8a** and **8b**, as illustrated

above. In the gas phase, Karelson et al., using the DO2* model, found the C–O bond length in **8** increased by 0.098 Å on going from the gas phase into a solution with a dielectric constant ε of 78.4, which implies increased contribution from the zwitterionic mesomer.

Parchment et al. [271] have provided more recent calculations on the 3-hydroxypyrazole equilibrium at the ab initio level. They noted that tautomer **9**, which was not considered by Karelson et al. [268], is the lowest-energy tautomer in the gas phase at levels of theory (including AM1) up to MP4/6-31G**//HF/3-21G [271]. Although **8** is the dominant tautomer observed experimentally in aqueous solution, in the gas phase **8** is predicted to be nearly 9 kcal/mol less stable than **9** at the MP4 level [271]. Using a DO model with an unphysically small cavity radius of 2.5 Å, Parchment et al. [271] were able to reproduce at the ab initio level the AM1-DO prediction of Karelson et al. [268], namely that **8** is the most stable tautomer in aqueous solution. With this cavity, though, **8** is predicted to be better solvated than **9** by –22.2 kcal/mol [271]. This result is inconsistent with molecular dynamics simulations with explicit aqueous solvation [271], and with PCM and SCME calculations with more reasonable cavities [271]; these predict that **8** is only about 3 kcal/mol better solvated than **9**. In summary, the most complete models used by Parchment et al. do not lead to agreement with experiment

The comparisons made by Parchment et al. [271] illustrate the importance of combining electronic polarization effects with corrections for specific solvation effects. The latter are accounted for parametrically by the explicit simulation, but that procedure cannot explicitly account for the greater polarizability of tautomer **8**. The various SCRF models *do* indicate **8** to be more polarizable than any of the other tautomers, but polarization alone is not sufficient to shift the equilibrium to that experimentally observed. Were these two effects to be combined in a single theoretical model, a more accurate prediction of the experimental equilibrium would be expected.

4.2.1.3 Isoxazoles

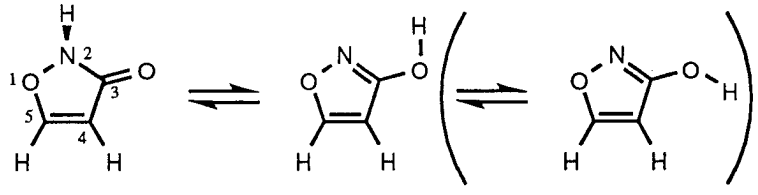

13 **14** **15**

Karelson et al. [268] used the AM1 DO2* method with a spherical cavity of 2.5 Å radius to study tautomeric equilibria in the 3-hydroxyisoxazole system (the keto tautomer **13** is referred to as an isoxazolone). AM1 predicts **13** to be 0.06 kcal/mol lower in energy than **14** in the gas phase. However, the AM1 dipole moments are 3.32 and 4.21 D for **13** and **14**, respectively. Hydroxy tautomer **14** is better solvated within the DO2* model, and is predicted to be 2.6 kcal/mol lower in energy than **13** in a continuum dielectric with $\varepsilon = 78.4$. Karelson et al. note, however, that the relative increase in dipole moment upon solvation is larger for **13** than for **14** (aqueous AM1 dipole moments of 5.05 and 5.39 D, respectively). This indicates that the relative magnitude of gas-phase dipole moments will not always be indicative of which tautomer will be better solvated within a DO solvation approach—the polarizability of the solutes must also be considered. In any case, the DO2* model is consistent with the experimental observation [266] of only the hydroxy tautomer in aqueous solution.

Woodcock et al. [272] also studied the 3-hydroxyisoxazole system, making several comparisons to the above work of Karelson et al. They noted in particular that the hydroxy tautomer has two possible rotamers about the C–O bond, one which places the hydroxyl proton syn to nitrogen (**14**) and one which places it anti (**15**). Karelson et al. considered only **14**, which is 4.3 kcal/mol lower in energy in the gas phase at the MP4/6-31G**//HF/3-21G level. Woodcock et al. also demonstrated that AM1 agrees poorly with this correlated ab initio level of theory for the relative energies of **13** and **14**: the MP4 calculations predict **13** to be 7.1 kcal/mol higher in energy than **14**. Finally, AM1 also disagrees with HF/6-31G**//HF/3-21G with respect to the molecular dipole moments. Tautomers **14** and **13** are predicted to have gas-phase dipole moments of 2.5 and 3.8 D respectively at the ab initio level, reversing the order found at the AM1 level. Moreover, the anti hydroxyl tautomer **15** has a gas-phase dipole moment of 6.2 D at the HF/6-31G**//HF/3-21G level! Thus, when Woodcock et al. considered the effects of solvation using a correct DO model (as opposed to DO2*) but continuing with the small spherical cavity radius of 2.5 Å used by Karelson et al., they find the relative energies in aqueous solution of **14**, **15**, and **13** to be 12.8, 0.0, and 1.8 kcal/mol respectively. Note the difference between AM1 and the ab initio level of theory with respect to **14** vs. **15**: the former predicts **15** to be the more stable tautomer by 2.6 kcal/mol while the latter predicts a reversal of this ordering by about 15 kcal/mol. Note as well that the relative energies of the two hydroxyl rotamers differ by 12.8 kcal/mol—this is a very large difference in electrostatic solvation free energies for rotamers, and, if we recall that the DO model calculates the free energy of solvation as being proportional to the square of the molecular dipole moment and inversely proportional to the cube of the

cavity radius., we can reasonable conclude that this large difference reflects both the problems of truncating the multipole expansion at the dipole and of choosing unreasonably small cavity radii.

Woodcock et al. also examined a different continuum model, namely the PCM model with a solvent accessible surface area defined according to the prescription of Aguilar and Olivares del Valle [273] based on basis set and partial atomic charge. This much more realistic cavity still predicts **13** to be better solvated than **14**, but by only 2.4 kcal/mol at the HF/6-31G**//HF/3-21G level. When combined with the MP4 gas phase energies, **14** is predicted to predominate by 4.7 kcal/mol. This is remarkably consistent with molecular dynamics simulation studies carried out by Woodcock et al. using frozen ab initio geometries for the solutes, solute partial atomic charges derived from electrostatic potential fitting [274], and the Transferable Intermolecular Potential 3-Point (TIP3P) [275] water model with the AMBER [276] force field. The simulations predict **13** to be better solvated than **14** by 2.2 ± 0.4 kcal/mol. They also make the much more reasonable prediction that the difference in solvation free energies for the two hydroxyl rotamers is only 1.7 ± 0.5 kcal/mol, favoring the anti rotamer. When either the PCM or the MD solvation results are added to the MP4 relative gas-phase energies, **14** is predicted to be the most stable in aqueous solution.

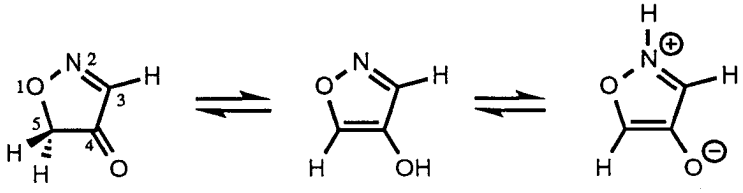

16 **17** **18**

Karelson et al. [268] used the AM1 DO2* method with a spherical cavity of 2.5 Å radius to study tautomeric equilibria in the 4-hydroxyisoxazole system (they did not specify which hydroxyl rotamer they examined). Tautomer **17** predominates in aqueous solution. Although AM1 predicts **16** to be about 10 kcal/mol more stable in the gas-phase than **17**, its dipole moment is only predicted to be 0.68 D. Tautomer **17** has a predicted dipole moment of 2.83 D in the gas-phase. With the small cavity, the two dipole moments increase to 0.90 and 4.56 D, respectively, and this is sufficient to make **17** 0.3 kcal/mol more stable than **16** in solution. Zwitterion **18** is much better solvated than either of the other two tautomers, but AM1 predicts its gas-phase relative energy to be so high that it plays no equilibrium role in either the gas phase of solution.

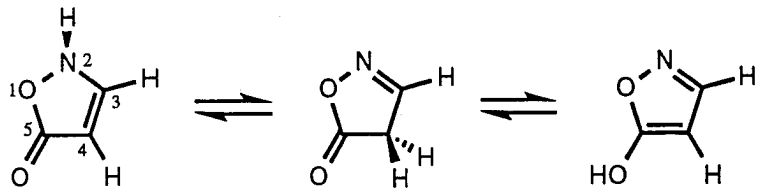

19 **20** **21**

The present authors have discussed the 5-hydroxyisoxazole tautomeric equilibrium at length in a previous review [83]. For the sake of completeness, we note that Karelson et al. [268] studied this equilibrium with the DO2* model and a spherical cavity radius of 2.5 Å and came to the conclusion that **19** should slightly predominate (hydroxyl rotation in **21** was not specified). Woodcock et al. [272] found that AM1 gas-phase energies differed from MP4/6-31G**//HF/3-21G energies by up to 5 kcal/mol, although predicted dipole moments were in better agreement between the two levels of theory than was the case for 3-hydroxyisoxazole (vide supra). Although Woodcock et al. found that adding solvation free energies from an ab initio DO model with a 2.5 Å spherical cavity radius also predicted that **19** should slightly predominate, this was not consistent with either PCM results or MD simulations, both of which suggested **20** to be lower in energy in aqueous solution. The present authors [277] employed ab initio levels of theory that effectively converged the gas-phase relative energies, noting, as had Rzepa et al. [270], that inaccurate geometries had been used for **19** in the earlier studies. When SM*x* solvation free energies were added to these gas-phase energies, the present authors predicted that both isoxazolone tautomers should be present with **20** slightly predominating. This is consistent with trends apparent in the tautomeric equilibria of the 3-methyl, 4-methyl, and 3,4-dimethyl homologs of this heterocyclic system, for which experimental equilibrium data are available [278, 279], and for which the SM*x* models are in good agreement with experiment [277]. Gould and Hillier [280] subsequently revisited this system and illustrated that the DO model was incapable of providing accurate predictions even when accurate geometries and a more reasonable cavity were employed. However, when higher solute multipole moments were included in the reaction field, the results were more consistent with the SM*x* predictions for the unsubstituted system. Finally, both the present authors as well as Gould and Hillier emphasized the importance of accounting for non-electrostatic components of the free energy of solvation.

4.2.1.4 Oxazoles

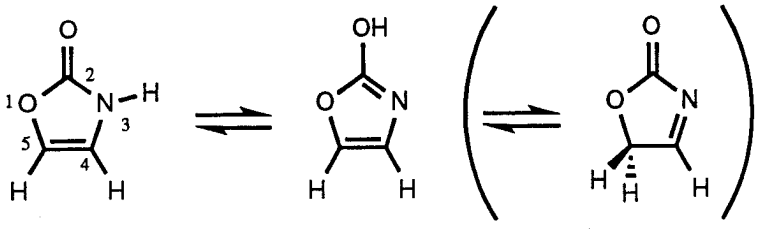

22 **23** **24**

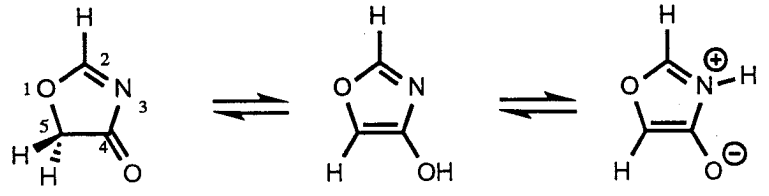

25 **26** **27**

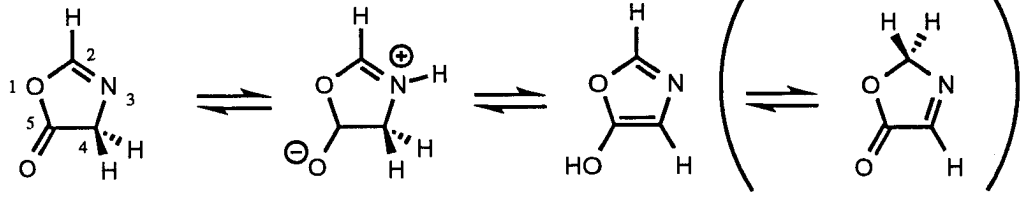

28 **29** **30** **31**

Karelson et al. [268] used the AM1 DO2* method with a spherical cavity of 2.5 Å radius to study tautomeric equilibria in the 2-, 4-, and 5-hydroxyoxazole systems (the keto tautomers are referred to as oxazolones). Tautomers illustrated above in parentheses were not considered and hydroxyl rotamers were not specified. In the first two systems, tautomers **22** and **25** are predicted by AM1 to be about 14 kcal/mol more stable than the nearest other tautomer in their respective equilibria. Differences in tautomer solvation free energies do not overcome this gas-phase preference in either case, and the oxazolones are predicted to dominate the aqueous equilibrium, as is observed experimentally [266].

In the 5-hydroxyoxazole system, AM1 predicts the 5-(4*H*)-oxazolone tautomer **28** to be the lowest in energy in the gas phase by 12.4 kcal/mol. This tautomer is experimentally observed in the solid state [266]. The employed DO2*

model, however, predicts that the zwitterionic tautomer **29** should predominate in aqueous solution by about 20 kcal/mol with a solvation free energy of nearly –40 kcal/mol; this is probably a large overestimation of the magnitude owing to the arbitrarily small size of the DO2* cavity employed. Experimental solution data are not available. The AM1 gas-phase energies are also not quantitative, suggesting that this might be an interesting system for which to make higher level predictions.

4.2.1.5 Triazoles

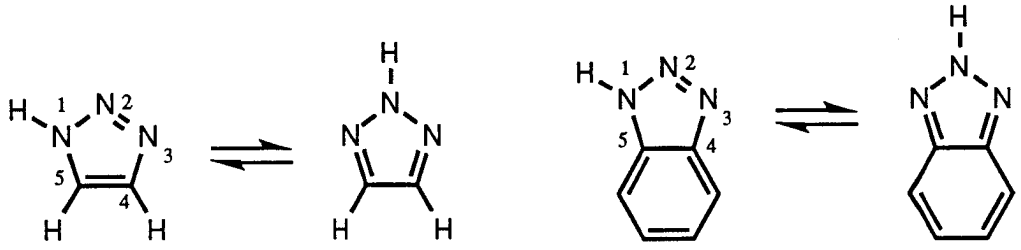

32 **33** **34** **35**

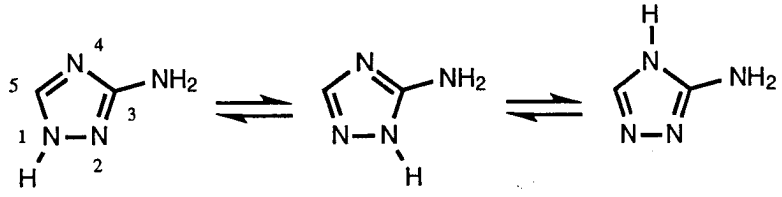

36 **37** **38**

Tomás et al. [281] have calculated the tautomeric equilibrium of 1,2,3-benzotriazole in the gas phase and compared their results to experimental data [282] derived from ultraviolet spectroscopy. Experiment suggests that **35** is about 4 kcal/mol more stable than **34**; this result is consistent with calculations [281] at the MP2/6-31G* level, which predict **35** to be 2.5 kcal/mol more stable than **34**. The same level of theory predicts **33** to be 5.0 kcal/mol more stable than **32** in the parent triazole system. Although experimental data are available indicating **35** to be the dominant tautomer in $CDCl_3$ and d_6-dimethyl sulfoxide solutions [279, 283], this equilibrium does not appear to have been the subject of any modeling, continuum or otherwise. It may prove to be somewhat challenging, however. Tomás et al. point out that correlation effects favor **35** by about 5 kcal/mol at the MP2 level; AM1, PM3, and HF calculations with moderate basis sets all predict

34 to be the lowest in energy in the gas phase. Moreover, Fabian [284] has noted significant discrepancies between experimental tautomeric equilibria and predictions from both AM1 and PM3 when one or more tautomers has adjacent pyridine-like lone pairs, as is the case for **34**. This suggests that the electronic densities calculated at these levels may not be sufficiently accurate for solvation modeling.

In conjunction with the present review we have carried out AM1-SM4 calculations in solvent *n*-hexadecane ($\varepsilon = 2.06$) for the benzotriazole equilibrium. We find that **35** is better solvated than **34** by 0.9 kcal/mol, with all of the differential solvation being found in the ΔG_{ENP} term. Not surprisingly, PM3-SM4 results are very similar. This seems to be out of step with the data from $CDCl_3$, the most nonpolar solvent for which experimental results are available. It is not clear, however, whether this difference is attributable to (i) the smaller dielectric constant of *n*-hexadecane compared to $CDCl_3$ (for $CHCl_3$ $\varepsilon = 4.8$ at 293 K [240]), (ii) specific interactions between weakly acidic chloroform and the basic benzotriazole tautomers, (iii) inadequacies in the semiempirical electronic structure, (iv) inadequacies in the SM4 model, or (v) some combination of any or all of the above. When SM5 models are available for $CHCl_3$ and DMSO, it will be interesting to revisit this system.

Another challenging triazole system, 3-amino-1,2,4-triazole, has been discussed by Parchment et al. [285]. In aqueous solution, ^{15}N-NMR indicates [286] a 2:1 mixture of **37**:**36**, with no detectable amounts of **38** present. Tautomer **38** is the least stable in the gas phase: at the CCSD/6-31G*//HF/6-31G* level, **36**, **37**, and **38** are predicted to have relative energies of 0.0, 0.4, and 7.8 kcal/mol, respectively [285]. With a DO model using a cavity radius of 3.0 Å at the HF/6-31G** level, Parchment et al. [285] predicted the relative energies of **36**, **37**, and **38** in aqueous solution to be 2.5, 0.0, and 1.4 kcal/mol, respectively; although the relative ordering of **36** and **37** is correct, **38** is too low in energy based on the above NMR data. PCM calculations at the same level of theory predicted the relative energies of **36**, **37**, and **38** in aqueous solution to be 0.0, 1.8, and 5.0 kcal/mol, respectively. This prediction of the electrostatics is more consistent with the observed equilibrium, and it appears that correcting for specific solvation effects could easily reverse the relative energies of **36** and **37**. However, it may be that the proximity of the primary and secondary amino functionality in tautomer **37** requires inclusion of a specific water molecule in the continuum calculation as there is an opportunity for a unique hydrogen bonding pattern possible only for that tautomer (each amino group hydrogen bonding to one lone pair of a single water molecule).

4.2.1.6 Tetrazoles

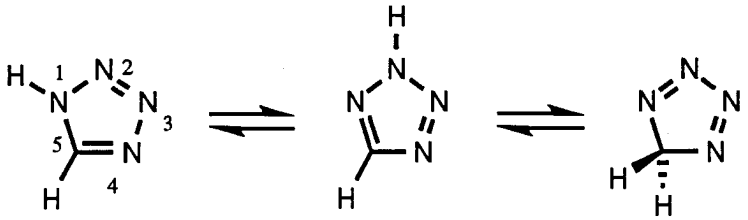

39 **40** **41**

Tetrazole can exist as three tautomers, as illustrated above. Wong et al. [287] have summarized the experimental and theoretical data for the gas-phase equilibrium; there is general agreement that **40** is more stable than **39** by about 2 kcal/mol, while **41** is about 20 kcal/mol higher in free energy. Wong et al. also used the DO3 model to examine electrostatic solvation effects on the tetrazole equilibrium at the MP2/6-311+G**//HF/6-31G* level. At this level they predict the equilibrium to barely reverse in a continuum dielectric of $\varepsilon = 2$, so that **39** is favored over **40** by about 0.1 kcal/mol. For $\varepsilon = 40$, they predict **39** to be favored over **40** by about 3 kcal/mol. This ordering is consistent with the experimental observation [283] of only **39** in dimethylsulfoxide ($\varepsilon = 46.5$ at 298 K [240]). The possible differential effects of specific interactions between tetrazole tautomers acting as hydrogen-bond donors to DMSO were not considered. Tautomer **41** remained much higher in energy for both dielectric constants.

For comparison purposes, we have carried out for the present review AM1-SM4 calculations in *n*-hexadecane ($\varepsilon = 2.06$). We find the solvation free energies of **39** and **40** to be –3.5 and –2.7 kcal/mol, respectively. Thus, the two solvation models agree that **39** is better solvated than **40**. However, we calculate the differential solvation free energy, 0.8 kcal/mol, to be smaller than that found by Wong et al., 2.0 kcal/mol (in a hypothetical solvent with $\varepsilon = 2.0$). Moreover, we calculate ΔG_{ENP} for **39** and **40** to be –4.4 and –3.6 kcal/mol, respectively. These values may be compared to the DO3 (also electrostatics only) results of Wong et al., which were –2.4 and –0.4 kcal/mol. These differences, as noted above for the 5-hydroxyisoxazole system, are probably attributable to the failure of the DO model to take account of higher multipole moments. The net result is that the two models differ for $\varepsilon = 2$—the DO3 model predicts a very slight prevalence of **39**, while the SM4 model predicts about a 7:1 ratio of **40**:**39**. Unfortunately, limited solubility of tetrazole in solvents less polar than DMSO has not yet permitted an experimental measurement of this equilibrium.

4.2.1.7 Pyridines

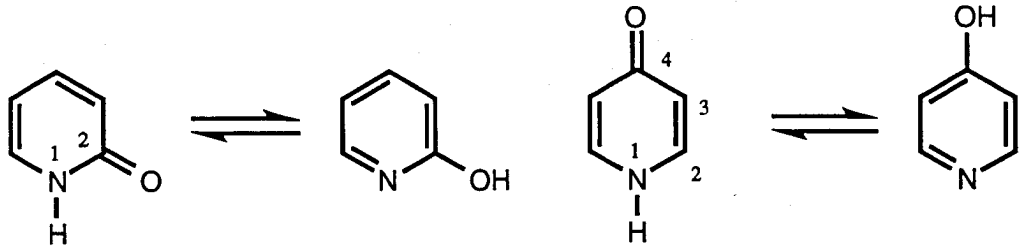

42 **43** **44** **45**

Hydroxypyridine/pyridone equilibria have been extensively studied. Numerous experimental [240, 266, 288, 289] and modeling studies of these systems in the gas phase [284, 290-293] and in solution [157, 159, 160, 195, 236, 260, 294-300] have appeared. An earlier review [83] by the present authors includes a summary of the literature through 1993. We briefly review that earlier work and include some more recent contributions.

The 2-substituted system has proven especially attractive to modelers because the experimental equilibrium constants are known both in the gas phase and in many different solutions. As a result, the focus of the modeling study can be on the straightforward calculation of the differential solvation free energy of the two tautomers, without any requirement to first accurately calculate the relative tautomeric free energies in the gas phase. However, in 1992 Les et al. [290] suggested that prior experimental data [240, 266, 288], primarily in the form of ultraviolet spectra in the gas phase and in low-temperature matrices, had been misinterpreted and that the reported equilibrium constants referred to homomeric dimers of tautomers (i.e., $(\mathbf{42})_2 \rightleftharpoons (\mathbf{43})_2$). Parchment et al. [291] contested this assertion and suggested an incomplete accounting for correlation in the modeling studies of Les et al. Simultaneously, a gas-phase microwave experiment appeared that unambiguously established the two tautomers to be monomeric in the gas phase [289].

Calculations on the differential solvation free energies of the two relevant tautomers are presented in the following table for several different models implemented at a number of levels of theory. The following discussion will focus on comparing specific calculations in the table.

We begin with a comparison of the various DO models to each other. Based on a parametric procedure that takes account of the molecular volume encompassed by the 0.001 a.u. electron density envelope, Wong et al. [297] suggested that an appropriate spherical cavity radius is 3.8 Å. Szafran et al. [157]

TABLE III

Differential free energies of solvation (kcal/mol) for 2-pyridone **42** and 2-hydroxypyridine **43** for different dielectric constants and solvent models.[a]

	Dielectric Constant					
Model/Hamiltonian[b]	ε = 2	ε = 5	ε = 36	ε = 78	Cavity	Ref
DO2*/AM1				4.3	rad. 3.15 Å[c]	[295]
DO2*/AM1	0.8	1.5	2.0	2.1	rad. 3.8 Å	[157]
DO2*/PM3	0.7	1.3	1.8	1.9	rad. 3.8 Å	[157]
DO2*/AM1[d]				1.5	rad. 3.8 Å	[157]
DO2*/PM3[d]				1.7	rad. 3.8 Å	[157]
DO/AM1				4.8	rad. 3.0 Å	[159]
DO/AM1	0.9	1.6	2.3	2.3	rad. 3.8 Å	[157]
DO/PM3	0.7	1.4	2.0	2.1	rad. 3.8 Å	[157]
DO/AM1[d]				2.7	rad. 3.8 Å	[157]
DO/PM3[d]				2.4	rad. 3.8 Å	[157]
DO/HF/3-21G				5.7	rad. 3.8 Å	[298]
DO/HF/6-31G**	1.1		3.0		rad. 3.8 Å	[297]
DO/HF/6-31+G**	1.2		3.4		rad. 3.8 Å	[297]
DO/MP2/6-31+G**	1.0		3.2		rad. 3.8 Å	[297]
DO/VWN/DZP				6.4	rad. 3.8 Å	[160]
DO/BP/DZP				6.2	rad. 3.8 Å	[160]
SCME(l = 6)/HF/6-31G**	1.5		4.2	4.3	rad. 3.8 Å	[195]
SCME(l = 6)/HF/6-31G**	3.3		4.5	4.6	ellipsoidal	[195]
PCM/AM1	1.6	3.3	4.8	5.0	van der Waals	[301]
PCM/HF/6-311G**	2.6		5.7	5.8	van der Waals	[195]
AM1-SM4 cyclohexane[e]	0.6				van der Waals	*f*
PM3-SM4 cyclohexane[e]	1.6				van der Waals	*f*
AM1-SM1 water[e]				4.4	van der Waals	[260]
AM1-SM2 water[e]				2.6	van der Waals	[236]
PM3-SM3 water[e]				4.3	van der Waals	[236]
PCM8/ST/AM1 water				4.1	van der Waals	[207]
PCM8/ST/PM3 water				3.0	van der Waals	[207]
Experiment	**1.1**	**1.8**	**3.8**	**4.3**		[288]

[a] In every case, 2-pyridone is the better solvated isomer by the amount indicated. [b] See text for description of Hamiltonians/acronyms. [c] rad. denotes radius of a spherical cavity. [d] Includes one explicit water of hydration. [e] The SM*x* and PCM8/ST models include non-electrostatic effects; the other models do not. [f] This work.

arrived at a similar cavity radius based on van der Waals volumes of the solutes. At the semiempirical level, Szafran et al. [157] compared the DO2* model to the normal DO approach. Although the DO2* model does not polarize the wave function as much as the full DO model, the effect on the differential solvation energy is fairly small at the AM1 and PM3 levels, amounting to only 0.2 kcal/mol at $\varepsilon = 78$. The agreement with experiment is good for the two smallest dielectric constants and rather poor for the two largest dielectric constants. When the cavity radius is treated as a free parameter, it is of course possible to improve the agreement with experiment for $\varepsilon = 78$. Karelson et al. [295] and Freitas et al. [159] chose unrealistically small cavity radii (2.5 Å) for their DO2* and DO calculations, respectively, at the AM1 level, and were able to increase the differential solvation free energy to more than 4 kcal/mol. Using the more reasonable cavity radius of 3.8 Å, Szafran et al. [157] considered the addition of one explicit water molecule. It is not clear, however, what the differential solvation energy of the monohydrates should be, since the tautomeric equilibrium constant for the monohydrates in the gas phase is not known (at the AM1 and PM3 levels, Szafran et al. found the monohydration energies to be identical for both tautomers—ab initio results focusing on the monohydrates in the gas phase have also appeared [293, 298-300]). What is noteworthy about the monohydrate calculations is that the difference between the DO2* and DO models becomes considerably more pronounced—the differential solvation energy differs by almost a factor of 2 at the AM1 level.

At ab initio levels of theory, Wong et al. [297] examined the effects of basis set and correlation (evaluated at the MP2 level) on the differential solvation free energy at $\varepsilon = 2$ and $\varepsilon = 36$. They did not calculate the $\varepsilon = 78$ case, noting that specific interactions not accounted for by the continuum model might be expected to be significant in aqueous solution. Within the DO model, however, the difference between $\varepsilon = 36$ and $\varepsilon = 78$ is almost negligible, as can be seen from many of the other calculations. In any case, Wong et al. achieve excellent agreement with experiment for $\varepsilon = 2$ and somewhat underestimate the differential solvation free energy for $\varepsilon = 36$. The effects of adding diffuse basis functions and taking account of electron correlation at the MP2 level are fairly small: each changes the differential solvation free energy by about 10%, albeit in opposite directions. Barone and Adamo [298] use the same cavity radius as Wong et al., (3.8 Å) but obtain a much larger differential solvation free energy at $\varepsilon = 78$, 5.7 kcal/mol, than would be expected based on the HF results of Wong et al. at $\varepsilon = 36$. The situation is not entirely clear, since the paper of Barone and Adamo states the calculation to be at the HF/3-21G level, while another paper by Adamo and Lelj [160] refers to this result as being at the HF/6-31G** level, which should

certainly agree closely with the results of Wong et al. at $\varepsilon = 36$. Assuming the calculations to be at the HF/3-21G level, it appears more likely that the discrepancy arises from the lack of polarization functions in the smaller basis set, since the reported geometries do not differ markedly. This seems to suggest a potentially important point, namely that at ab initio levels polarization basis functions appear to be crucial in permitting a realistic relaxation of the solute wave function in the presence of a reaction field. Adamo and Lelj [160] found a similarly large differential solvation free energy for $\varepsilon = 78$ using density functional theory (DFT). In this case, the local density approximation of Vosko, Wilks, and Nusair [302] (VWN) was used; the nonlocal corrections of Becke [303] and Perdew [304] for exchange and correlation energy, respectively (BP), were also employed. In both cases the results significantly overshoot the aqueous experimental values. Hall et al. [292] have found very similar density functional approaches to do poorly with respect to prediction of the gas-phase tautomeric equilibrium constant, so it appears that the DFT density for one (or both) of the two tautomers is inaccurate.

Young et al. [195] have provided a calculation in which they compared expanding the multipole series up to $l = 6$ in a spherical cavity of 3.8 Å. These results may be compared directly to those of Wong et al. [297] at the identical level of theory/basis set in order to assess the effect of including higher moments. In each case, the differential solvation free energy increases by about 40%. This illustrates nicely the relationship between cavity radius and model approximations—it is apparent that the prescription used by Wong et al. to calculate cavity radii may be useful when the effects of higher multipole moments are ignored (i.e., for a DO model) but it will *not* necessarily be useful for more general reaction field approaches. In this case, inclusion of higher order multipoles improves agreement with experiment for $\varepsilon = 36$ but agreement is now less good for $\varepsilon = 2$. As noted earlier, there is effectively no difference between the results for $\varepsilon = 78$ and $\varepsilon = 36$—for a cavity radius of 3.8 Å, the former are in quantitative agreement with experiment. Upon switching from a spherical cavity to an ellipsoidal one, however, the agreement with experiment is degraded [195], especially for $\varepsilon = 2$. This is in opposition to the general observation that ellipsoidal cavities are to be preferred over spherical ones (although both are inferior to more general cavities).

Results for continuum models having more general cavities are available. In particular, Wang and Ford [301] and Young et al. [195] have carried out PCM calculations at the AM1 and HF/6-311G** levels, respectively. Both sets of calculations significantly overestimate the differential solvation free energies. This may reflect a difficulty with charge penetration outside the cavity.

The GB/ST-type SM*x* models also employ a general cavity. Since they include non-electrostatic effects, they require parameterization on a solvent-by-solvent basis, and at present results for 2-pyridone are only available for $\varepsilon = 2$ (using the SM4 cyclohexane model [217]) and $\varepsilon = 78$ (using the SM1 [210], SM2 [211], and SM3 [212] water models). The cyclohexane solvation model brackets the experimental result depending on whether the AM1 or PM3 Hamiltonian is used. This is somewhat surprising, since the CM1 charge models should minimize differences between the two Hamiltonians. Indeed, for the pyridones the AM1-CM1 and PM3-CM1 atomic partial charges are very similar and the absolute solvation free energies agree closely (–6.7 and –6.9 kcal/mol for AM1-SM4 and PM3-SM4 cyclohexane, respectively). For 2-hydroxypyridine, the charges remain quite similar; the largest deviation is 0.06 charge units on the pyridine nitrogen (–0.53 with AM1-CM1 and –0.47 with PM3-CM1). Nevertheless, the solvation of this tautomer appears very sensitive to these small charge differences, and the absolute free energies of solvation are –6.1 and –5.3 kcal/mol for AM1-SM4 and PM3-SM4 cyclohexane, respectively. This effect is discussed in somewhat more detail for formamidic acid in section 4.2.2.1. Non-electrostatic contributions to the differential solvation free energy, as measured by G^{o}_{CDS} values, are less than 0.1 kcal/mol. This is intuitively reasonable and consistent with the assumptions of the electrostatics-only continuum studies.

The aqueous solvation results are in good agreement with experiment for the SM1 and SM3 models, but quantitatively too small for the SM2 model. The present authors have provided a detailed analysis of these results that emphasizes the importance of (i) relaxing the electronic wave function in the presence of the reaction field and (ii) reoptimizing the geometry in the presence of the reaction field [236]. The latter effect is small in terms of changes in bond lengths, angles, etc.; but, it permits additional electronic relaxation which contributes to the overall solvation free energy.

Using the PCM8/ST model, Orozco et al. [207] arrive at values similar to those found by the SM*x* models. Interestingly, in this case it is the AM1-based model that is more accurate than the PM3-based one. This illustrates the subtle balancing that goes into the parameterization of models that include electrostatic and non-electrostatic effects simultaneously.

One point of particular interest is that it is not clear from the electrostatics-only models whether non-electrostatic phenomena affect the *aqueous* tautomeric equilibria. For instance, the DO results of Wong et al. [297] would suggest there are differentiating non-electrostatic phenomena, while the results of Young et al. [195] for a multipole expansion in a spherical cavity suggest that there are not. Since the SM1, SM2, and SM3 GB/ST models use Mulliken charges rather than

CM1 charges in the calculation of ΔG_{ENP}, corrections for charge inadequacies appear in G^{o}_{CDS} and it is not possible to separate the electrostatic and non-electrostatic components of the free energy of solvation.

Finally, we note that Karelson et al. [295] have used the DO2* model with small cavity radii to consider aqueous solvation effects on other tautomeric equilibria of substituted pyridines. In particular, they examined methyl/methylene, amino/imino, hydroxy/oxo, and mercapto/thiono substitution at the 2-, 3, and 4-positions of pyridine. They observed methyl/methylene equilibria to be only slightly perturbed by aqueous solvation. Amino/imino equilibria were slightly more perturbed, followed by hydroxy/oxo equilibria. Mercapto/thiono equilibria were *very* significantly affected by aqueous solvation; Karelson et al. predicted pK shifts of up to 16 units. This sensitivity of the thiono group to solvation is also discussed in the next section. Overall, the tautomeric equilibria of 3- and 4-substituted pyridines were more sensitive to aqueous solvation than were those of 2-substituted pyridines.

4.2.1.8 Pyrimidines, Purines, and Nucleic Acid Bases

adenine

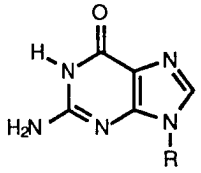

guanine

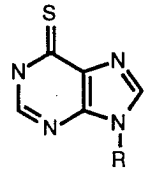

6-thiopurine

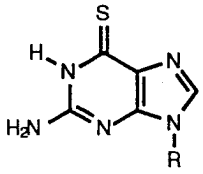

6-thioguanine

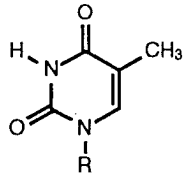

thymine

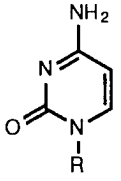

cytosine

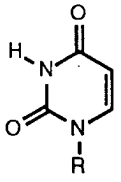

uracil

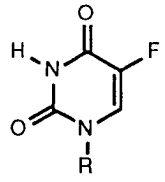

5-fluorouracil

Some of the impetus for studying tautomeric equilibria in heterocycles arises because of the postulate that point mutations in genetic material may be introduced when a given base exists in a tautomeric form during replication [279, 305-307]. Cytosine, in particular, has imino and hydroxy tautomers that are within 3 kcal/mol of the global minimum illustrated above (because of the very large number of possible tautomers for the purines and pyrimidines, only the lowest energy tautomers are presented). This analysis has been made based on a

combination of matrix infrared spectroscopy [308] and theoretical [309-313] (gas phase) results. In the latter case, it is worth noting that Estrin et al. [314] found both local and gradient-corrected implementations of density functional theory to be effective in computing the relative tautomeric energies. This is in contrast to the observations of Hall et al. [292], discussed in the previous section, with respect to 2-pyridone. Even for the other nucleic acid bases, there has been interest in the possibility that solvation might influence the tautomeric equilibrium sufficiently to play a role in biological systems.

Continuum models have been employed by a number of groups in an effort to address this question. Scanlan and Hillier [309] considered the effect of aqueous solvation on uracil, thymine, 5-fluorouracil, and cytosine using a non-self-consistent DO reaction field model and HF/3-21G electronic structures. They observed that the model gave qualitative agreement with experimental results for solvation effects on the tautomeric equilibria, but that the predicted aqueous populations of non-standard tautomers were too small to be consistent with the observed rates of mutation in DNA replication. They concluded that other factors associated with the macromolecular system could not be ignored in this regard. Katritzky and Karelson [315] used the DO2* model with the AM1 and PM3 Hamiltonians to evaluate tautomeric equilibria for all of the nucleic acid bases, as well as for the 1-methylated pyrimidine bases. Cavity radii ranged from 3.45 to 3.83 Å for the pyrimidines, and the qualitative results were reported to be insensitive to 10% changes in these values; cavity radii were not reported for the purines. Katritzky and Karelson emphasized that the semiempirical dipole moments were in good agreement with experiment for uracil and thymine, and that the semiempirical structures also agreed well with higher level ab initio results. Similar points have been made by Fabian with respect to the success of semiempirical levels of theory in predicting the geometries and dipole moments for these and related heterocycles [284]. Katritzky and Karelson provide detailed comparisons between theory and experiment for the relative tautomeric energies of each base. Although uncertainties in some of the experimental relative free energies are quite large, nevertheless, the DO2* results were in quite reasonable qualitative agreement.

Young et al. [316] examined the cytosine tautomeric equilibrium using both the DO model (cavity radius of 3.54 Å) and a multipole expansion through $l = 6$ in both spherical and ellipsoidal cavities. They also employed the PCM model. All of their results were at the HF/6-31G** level. They observed that the absolute free energies of solvation were quite sensitive to choice of model, but that relative free energies were much less sensitive. They also noted that only the DO model gave good agreement with experimental estimates for the solvation

free energy of a high-energy oxo-amino tautomer. Finally, they noted that in some cases the AM1 results of Katritzky and Karelson benefited from a cancellation of errors in the gas phase and solvation energies. Ford and Wang [178] also examined the solvation of the three lowest energy tautomers of cytosine using an AM1 PCM model, and arrived at similar conclusions to those discussed above.

Orozco and Luque [317] have examined the tautomerism and protonation of 7-aminopyrazolopyrimidine (a drug component resembling adenine) using free energy perturbation and the SM2, PCM9/ST, and PCM10/ST continuum models. In this case, they note good agreement between the ab initio PCM9/ST model and their simulations with respect to which tautomer is the best solvated. This appears to be supported by experimental data. The AM1-based SM2 and PCM10/ST results, on the other hand, predict a different tautomer to be better solvated, apparently illustrating a case where the semiempirical wavefunction fails to provide an adequate representation of the solute electronic structure.

Lastly, some studies have recently appeared examining thiosubstituted purines (commonly used in the treatment of human leukemia) and thiopyrimidines. In particular, Contreras and Alderte [318] used the AM1-SM1 model to examine the tautomeric equilibrium of 6-thiopurine, and Alhambra et al. [319] used an HF/6-31G* PCM model to examine the tautomeric equilibrium of 6-thioguanine. Both studies noted very large polarization free energies associated with thiono tautomers, the net effect being a large shift of negative charge onto sulfur and a corresponding large gain in solvation free energy. These observations are consistent with the results of Karelson et al. [295] for thiosubstituted pyridines. In each case, aqueous solvation reversed the relative stability of the lowest energy thiol and thiono tautomers compared to the gas phase. Alhambra et al. also considered the solvation of protonated forms of 6-thioguanine [319]. Contreras and Alderete [320, 321] calculated free energies of solvation of prototropic tautomers of 2-thiopyrimidine using the SM2 and DO models. They found considerably larger solvation energies for the thione than the thiol by both approaches.

4.2.2 Non-heterocyclic Tautomeric Equilibria

In addition to heterocycles, other molecular systems have attracted theoretical attention with respect to prediction of tautomeric equilibria and solvation effects thereon. The most commonly studied example in this class is the equilibrium between formamide and formamidic acid, discussed in the next section. In addition, some continuum modeling of solvation effects on keto/enol equilibria have appeared; these are presented in section 4.2.2.2. We note that the equilibrium

between glycine and its zwitterionic form, discussed in section 4.1.1, is also formally a tautomeric equilibrium.

4.2.2.1 Formamide

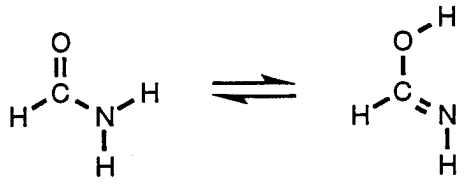

46 **47**

High-level gas-phase calculations unambiguously establish formamide **46** to be roughly 13 kcal/mol more stable than formamidic acid **47** [198, 297, 322]. It will be noted that these molecules represent the critical "fragment" of 2-pyridone involved in that molecule's tautomeric equilibrium. As such, it comes as no surprise that modeling of solvation effects indicates the amide form to be further stabilized in solution [198, 297]. As a result, no experimental data are available to which to compare. It remains instructive, however, to compare different theoretical studies. Wong et al. [297] used the DO model with a spherical cavity radius of 3.15 Å at the QCISD/6-31+G** level and concluded that the amide tautomer had the larger electrostatic free energy of solvation by 1.5 and 4.1 kcal/mol for dielectric constants of 2 and 36, respectively. Sato and Kato [198] also examined this system using a multicenter multipole expansion within a spherical cavity of radius 3.7 Å. These authors concluded that the amide tautomer had the larger electrostatic free energy of solvation by only 2.3 kcal/mol for a dielectric constant of 36 ($\varepsilon = 2$ was not examined). The reduction in magnitude of the differential solvation free energy may be a manifestation of either the more complete multipole expansion favoring the imine tautomer (which has a smaller dipole moment), or the considerably larger cavity radius employed, or both. The cavity radius is probably playing a significant role, since Wong et al. found ΔG_{ENP} ($\varepsilon = 36$) for formamide to be –4.3 kcal/mol, while Sato and Kato [198], with a more complete multipole expansion, obtained a value of only –2.8 kcal/mol.

For the present review we examined the $\varepsilon = 2$ case using the PM3-SM4 *n*-hexadecane model. This model is particularly appropriate because the PM3-CM1 dipole moments (3.4 and 1.2 D for formamide and formamidic acid, respectively) agree well with values obtained from MP2/6-31G** wave functions (3.9 and 1.2 D, respectively) [235]. The predicted differential free energy of

solvation is 1.9 kcal/mol, which is fairly close to the value obtained by Wong et al. [297]. However, the PM3-SM4 model predicts ΔG_{ENP} to be –4.4 kcal/mol at $\varepsilon = 2$; the DO model of Wong et al. [297] predicts a value of only –1.7 kcal/mol. Evidently, although solvation terms arising from multipole moments larger than the dipole and/or the approximation of a spherical cavity are not small, they appear to cancel in the differential free energy calculation. The PM3-SM4 results predict the change in G^{o}_{CDS} to be 0.3 kcal/mol on going from formamide to formamidic acid, a not entirely negligible change.

Finally, we note that the AM1-SM4 model is less satisfactory for this problem (predicted differential free energy of –0.2 kcal/mol in *n*-hexadecane), apparently because it overestimates the polarity of the functional groups in formamidic acid, especially the imine group (the AM1-CM1 dipole moment is 1.7 D and the atomic partial charges are up to 0.2 units larger than found for PM3-CM1). This deficiency is probably also reflected in the AM1-SM4 underestimation of solvation effects at $\varepsilon = 2$ for the 2-pyridone/hydroxypyridine tautomeric equilibrium discussed above. The greater generality of the PM3-CM1 model for nitrogen-containing systems has been previously noted [235].

4.2.2.2 Keto/enol equilibria

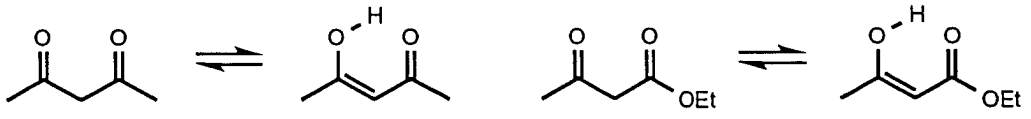

48 **49** **50** **51**

Substantial populations of intramolecularly hydrogen bonded enol tautomers of β-diketones and β-ketoesters are found in the gas-phase and in nonpolar solvents [240]. In water, on the other hand, the dione form is better solvated than the enol, causing the equilibrium to shift; for example, for ethyl 3-oxobutanoate **50**, the differential free energy of aqueous solvation for the two tautomers is 1.4 kcal/mol [323, 324]. The present authors examined this equilibrium with the SM1, SM2, and SM3 aqueous solvation models and found the differential free energies of solvation to be 1.1, –1.2, and 1.2 kcal/mol, respectively [236, 260]. The sizable difference between the predictions of the SM2 and SM3 models, with the latter being in much better agreement with experiment, arises from the ΔG_{ENP} term of the enol, which is very sensitive to the partial atomic charges on the oxygen atoms and on the hydroxyl proton. For 2,4-pentanedione, the differential free energy of aqueous solvation favors the dione tautomer **48** by 2.4 kcal/mol [323, 324] (note that a tabulation error occurred in our earlier work [236, 260]; our previously

tabulated experimental value of 1.0 kcal/mol is for gas to dimethylsulfoxide, *not* to water). The SM1, SM2, and SM3 aqueous solvation models predict differential free energies of solvation of 0.9, –1.6, and 0.6 kcal/mol, respectively [236, 260]. Again, the ΔG_{ENP} term of the enol **49** is very sensitive to variations in partial charges from the AM1 and PM3 Mulliken population analyses.

The 2,4-pentanedione system is interesting, since it seems to represent a challenge for the earlier generation SM*x* models. Moreover, data are also available for the tautomeric equilibrium constant in cyclohexane [324]. This allows us to explore the performance of the SM4 cyclohexane model, and the SM4-SRP water model (developed originally for hydrocarbons, ethers, and aldehydes [213], and later extended to include alcohols [325]; we observe that the performance of the SM4-SRP water model is about as good for ketones as for aldehydes). The situation is made particularly interesting because the direction of the equilibrium perturbation relative to the gas phase is opposite for the two solvents. In cyclohexane, the differential free energy of solvation for **48** and **49** is –0.7 kcal/mol (i.e., favoring **49**) while in water it is 2.4 kcal/mol (i.e., favoring **48**). Obviously, the differential free energy of transfer from cyclohexane to water favors **48** by 3.1 kcal/mol.

This system is ideal for illustrating many issues associated with continuum solvation modeling, and we note several points that particularly merit discussion. Table IV provides the relevant details of the calculations.

To begin, the shift of the equilibrium constant in one direction in cyclohexane, and in the other direction in water (relative to the gas phase) could arise from several different phenomena. For instance, it could be that the enol is more polar than the dione in the gas phase, but the dione is more polarizable than the enol. In such a situation, the low dielectric medium would not induce sufficient polarization in the dione, and ΔG_{ENP} would be larger for the more polar enol; in water, the greater polarizability of the dione would permit a reversal of the relative magnitudes of the two ΔG_{ENP} terms. This does not appear to be the case, however. Instead, ΔG_{ENP} favors the dione slightly in cyclohexane, and by a still larger margin in water, i.e., it is both more polar and more polarizable than the enol. Instead, focusing on the AM1-SM4 models, specific solvation effects associated with G^{o}_{CDS} sufficiently favor the enol in cyclohexane to overcome the small difference in ΔG_{ENP}. That preference is found entirely in the CD component; since the two tautomers are essentially equal in size, there is no distinction between them in the CS term. In the enol, there is a greater exposure of more polarizable (now in the sense of participating in favorable interactions

TABLE IV

Predicted solvation free energies and solvent-accessible surface areas (SASA) of 2,4-pentanedione tautomers in cyclohexane and water.[a,b]

	Dione **48**		Enol **49**	
	AM1	PM3	AM1	PM3
SM4 (cyclohexane)				
G_P	–3.0	–3.5	–2.4	–1.9
ΔE_{EN}	0.5	1.0	0.2	0.2
ΔG_{ENP}	–2.5	–2.5	–2.2	–1.7
G^o_{CD}	–17.0	–17.1	–17.5	–17.4
G^o_{CS}	14.8	14.8	14.8	14.7
G^o_{CDS}	–2.1	–2.3	–2.6	–2.7
ΔG^o_S	–4.6	–4.8	–4.8	–4.4
relative ΔG^o_S[c]	0.0	0.0	–0.2	0.4
SASA(CD)[d]	358.2	361.6	360.1	357.9
SASA(CS)[e]	596.0	593.9	596.7	591.6
SM4-SRP (water)				
G_P	–16.5	–16.1	–9.1	–7.7
ΔE_{EN}	7.8	6.9	2.2	1.7
ΔG_{ENP}	–8.7	–9.2	–6.9	–6.0
G^o_{CDS}	0.3	0.3	0.2	0.3
ΔG^o_S	–8.4	–8.9	–6.7	–5.7
relative ΔG^o_S	0.0	0.0	1.7	3.2
SASA[f]	304.6	304.8	300.8	298.2

[a] Free energies in kcal/mol. SASA in Å^2. [b] All geometries were fully optimized both in the gas phase and in solution. [c] Relative solvation free energy of dione and enol using the same NDDO Hamiltonian. [d] Solvent radius 2.0 Å for cavitation and dispersion. [e] Solvent radius 4.9 Å for cavitation and solvent structural rearrangement. [f] Solvent radius 1.4 Å.

associated with dispersion) hydrocarbon surface area at the expense of less polarizable oxygen surface area compared to the dione. This effect is worth about 0.4 kcal/mol favoring the enol in both of the SM4 models. In the AM1 case, that is sufficient to perturb the gas-phase equilibrium in the correct direction, although the magnitude of the perturbation is underestimated by about 0.5 kcal/mol. In the PM3 case, the difference in ΔG_{ENP} between the dione and the enol is larger, (apparently this term is quite sensitive to small charge variations in the enol—note that both SM4 models give much more consistent answers for the dione than the enol) and the net prediction is a very small shift of the gas-phase equilibrium in the wrong direction. Still, this is a fairly small quantitative error and the qualitative observation that these two terms are opposed remains unchanged.

While the PM3-SM4 model does appear to slightly underestimate the polarity of the enol component, there is some cancellation of errors upon considering the differential transfer free energies between cyclohexane and water. As noted above, experiment indicates that the differential free energy of transfer of the dione and the enol is 3.1 kcal/mol; the PM3-SM4 model predicts this value to be 2.8 kcal/mol, in excellent quantitative agreement. AM1-SM4 is less satisfactory in this regard, predicting only 1.9 kcal/mol.

Optimized 2,4-pentanedione geometries:

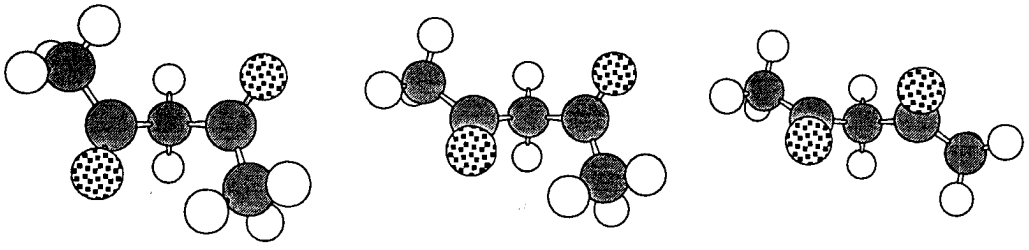

Gas phase **Cyclohexane** **Water**

The analysis is complicated, however, because the dione undergoes a dramatic change in geometry upon optimization in aqueous solution. As illustrated above, the dihedral angle between the planes containing the two carbonyl groups and their respective substituents changes from 137° in the gas phase, to 113° in cyclohexane, to 59° in water. Reducing this dihedral angle aligns the carbonyl bond dipoles (1.36, 1.43, and 1.92 D in the gas phase, cyclohexane and water, respectively, using AM1-CM1A [235] charges) and improves the solvation of this tautomer. Note that G_P is increased dramatically in water compared to the twofold increase one would expect over cyclohexane due to

polarizability and geometric relaxation. That geometry change comes at the cost of an increase in solute internal energy, reflected in ΔE_{EN} being a very sizable 7 to 8 kcal/mol for the two models. The quantity ΔE_{EN} is the difference in the expectation values of the *gas phase* Hamiltonian operating on the optimized gas-phase and solvated wavefunctions. That is the complicating factor in the differential free energy of solvation analysis, because it brings the gas-phase potential energy surface back into the problem. It is not at all clear that the semiempirical levels accurately represent the gas-phase energetics of the observed change in geometry, and this may result in quantitative differences between experiment and the two SM4 models. In any case, the 2,4-pentanedione system should be interesting to study with ab initio solvation models that employ levels of theory adequate for the gas-phase torsional aspect of the problem. It would also be of interest to see how well this large change in geometry is reproduced by models that employ idealized cavities compared to ones that more accurately represent the solute's shape.

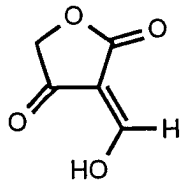

3-acetyltetronic acid

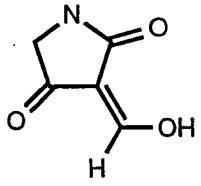

3-acetyltetramic acid

Finally, although they have not yet been the subject of any modeling study that has included solvation effects, 3-acetyltetronic and 3-acetyltetramic acid are very interesting solutes to consider. Each has more than 10 plausible tautomers—only the lowest-energy structures, as calculated at both the AM1 and MNDO levels by Broughton and Woodward [326], are shown above. The experimental situation in chloroform, as determined by NMR, remains unclear with respect to preferred structure. Gelin and Pollet [327] and Saito and Yamaguchi [328] have offered contrasting interpretations of the spectral data. Broughton and Woodward note that their semiempirical gas-phase calculations are in accord with the spectral interpretation of Gelin and Pollet, and as a consequence they suggest that solvation effects do not affect the tautomeric equilibrium. It seems evident that an investigation using a suitable chloroform continuum model would be worthwhile.

4.2.3 LACTOLIZATION

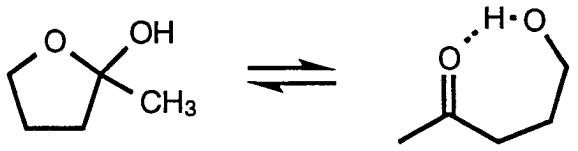

52 **53**

The present authors have examined the equilibrium between the lactol 2-hydroxy-2-methyltetrahydrofuran **52** and its corresponding open chain hydroxyketone **53** using the SM1, SM2, and SM3 models. The experimental situation indicates that the two structures are present in roughly equal proportions in non-polar media, while in water none of the lactol form is observed [329]. Making a reasonable assumption about detection limits, this sets a lower bound on the differential free energy of solvation for the two isomers of about 4 kcal/mol. Calculation of the differential free energy of transfer from the *gas phase* to aqueous solution using the SM1, SM2, and SM3 models gives values of 4.1, 3.6, and 4.4 kcal/mol, respectively. These results are probably somewhat too small since available experimental values are for the free energy of transfer from cyclohexane to water. Moreover, only one conformation of each tautomer was considered. For the hydroxyketone, the semiempirical models all predict the illustrated conformation having the intramolecular hydrogen bond to be lowest in energy, but this system should be revisited with an SM4 water model. Unfortunately, the gas-phase energies are required in order to calculate the free energy of transfer from one solvent to another when multiple conformations are involved, and this makes the problem somewhat more challenging.

5 Dynamic effects in kinetics and spectroscopy

The simplest generalization of free-energy-of-solvation concepts to dynamics in solution is provided by transition state theory. In conventional transition state theory, the rate constant of a chemical reaction at temperature T is given by

$$k(T) = \frac{k_B T}{h} K^{\neq,0} \exp[-\Delta G^{\neq,0}(T) / RT] \tag{59}$$

where k_B is Boltzmann's constant, h is Planck's constant, $K^{\neq,0}$ is unity for unimolecular reactions and the reciprocal of the standard state concentration for bimolecular reactions, and $\Delta G^{\neq,0}(T)$ is the standard-state free energy of

activation of the saddle point. For reactions in solution, $\Delta G^{\neq,0}(T)$ contains a solvation contribution which equals the free energy of solvation of the transition state minus the free energy of solvation of reactants [65-67]. To go beyond the conventional theory, we must define a reaction coordinate s and generalize the free energy of solvation to be a function of that coordinate; this is done by generalizing [330-333] the concept of potential of mean force [41, 82, 334-337] to treat generalized transition states defined at arbitrary locations along the reaction coordinate. The resulting standard-state free energy of activation as a function of s (called, for short, the free energy profile) is given by

$$\Delta G^{GT,0}(T,s) = \Delta G^{GT,0}_{solute}(T,s) + \Delta G^{0}_{S}(s,T) - \Delta G^{0}_{S}(R|T) \qquad (60)$$

where all quantities are standard-state ones at temperature T, and the first term on the right-hand side is the internal standard-state free energy of the solute at s, the second term is the free energy of solvation at s, and the third term is the free energy of solvation of the reactant species. Note that the last term is an equilibrium quantity, but $\Delta G^{0}_{S}(s,T)$ is a generalized equilibrium quantity (sometimes called a quasiequilibrium quantity) for any choice of s, even the gas-phase saddle point, because both the conventional and generalized transition states have one less degree of freedom than equilibrium species.

Even at this level of dynamical theory, one is not restricted to considering equilibrium solvation of the gas-phase saddle point or of configurations along the gas-phase reaction path [109, 338-344], and to the extent that the solvent is allowed to affect the choice of the reaction path itself, dynamic (i.e., nonequilibrium) solvation effects begin to appear in the theory.

To more fully appreciate the equilibrium models, like SCRF theories, and their usefulness and limitations for dynamics calculations we must consider three relevant times, the solvent relaxation time, the characteristic time for solute nuclear motion in the absence of coupling to the solvent, and the characteristic time scale of electronic motion. We treat each of these in turn.

First, consider the solvent. The characterization of the solute-solvent coupling by a relaxation time is based on analogy to Brownian motion, and the relaxation time is called the frictional relaxational time τ_F. It is the relaxation time for momentum decay of a Brownian motion in the solute coordinate of interest when it interacts with the solvent under consideration. If we call the subject solute coordinate s, then the component of frictional force along this coordinate may be written as

$$F_s = -\mu\varsigma\frac{ds}{dt} \tag{61}$$

where μ is the reduced mass for motion along coordinate s, ζ is the frictional constant, and t is time. Then the momentum (or velocity) for Brownian motion in coordinate s decays as [32, 345, 346] $e^{-\zeta t}$.

Writing the momentum decay function as e^{-t/τ_F} yields

$$\tau_F = \frac{1}{\varsigma}. \tag{62}$$

Even if we consider a single solvent, e.g., water, at a single temperature, say 298K, ζ depends on the solute and in fact on the coordinate of the solute which is under consideration, and we cannot take τ_F as a constant. Nevertheless, in the absence of a molecular dynamics simulation for the solute motion of interest, τ_F for polar solvents like water is often approximated by the Debye model. In this model, the dielectric polarization of the solvent relaxes as a single exponential with a relaxation time equal to the rotational (i.e., reorientational) relaxation time of a single molecule, which is called τ_D or the Debye time [32, 347]. The Debye time may be associated with the relaxation of the transverse component of the polarization field. However the solvent fluctuations and frictional relaxation occur on a faster scale given by [348, 349]

$$\tau_L = (\varepsilon_\infty/\varepsilon_0)\tau_D \tag{63}$$

where ε_∞ is the infinite-frequency relative permittivity, and ε_0 is the static (i.e., zero-frequency) relative permittivity. (At constant temperature and pressure, the relative permittivity is the dielectric constant.) The quantity τ_L is called the longitudinal relaxation time [350, 351]. Dielectric dispersion measurements [352] on water yield $\varepsilon_\infty = 1.8$, $\varepsilon_0 = 78.5$, and $\tau_D = 8.5$ ps, and hence $\tau_L = 0.2$ ps. Thus $\tau_F \cong 0.2$ ps.

Next consider the solute. We will again call the relevant solute nuclear coordinate s and the characteristic time now τ_s. For a thermally activated barrier crossing, where s is the reaction coordinate for passage over an effective potential $V_{\text{eff}}(s)$ at temperature T, a reasonable expression is

$$\tau_s = 1/\omega^{\ddagger} \tag{64}$$

where the barrier is written in the vicinity of its maximum as

$$V_{\text{eff}}(s) = V_{\max} - \frac{1}{2}\mu\left(\omega^{\ddagger}\right)^2 s^2. \tag{65}$$

Note that the imaginary frequency associated with such a barrier is $i\omega^{\ddagger}$. For a bound mode with frequency ω_{vib}, an analogous approximation would be

$$\tau_s = 1/\omega_{\text{vib}}. \tag{66}$$

The solute electronic time scale will be called τ_{elec}. It may be approximated as $h/\Delta E_1$, where ΔE_1 is the lowest (spin-allowed) electronic excitation energy of the solute.

A fully realistic picture of solvation would recognize that there is a distribution of solvent relaxation times (for several reasons, in particular because a second dispersion is often observable in the macroscopic dielectric loss spectra [353-355], because the friction constant for various types or modes of solute motion may be quite different, and because there is a fast electronic component to the solvent response along with the slower components due to vibration and reorientation of solvent molecules) and a distribution of solute electronic relaxation times (in the orbital picture, we recognize different lowest excitation energies for different orbitals). Nevertheless we can elucidate the essential physical issues by considering the three time scales τ_F, τ_S, and τ_{elec}.

The SCRF models assume that solvent response to the solute is dominated by motions that are slow on the solute electronic motion time scales, i.e., $\tau_F >> \tau_{\text{elec}}$. Thus, as explained in Section 2.1, the solvent "sees" the solute electrons only in an averaged way. If, in addition to the SCRF approximation, we make the usual Born-Oppenheimer approximation for the solute, then we have $\tau_s >> \tau_{\text{elect}}$. In this case the solute electronic motion is treated as adjusting adiabatically both to the solvent motion and to the solute nuclear motion.

For gas-phase molecules the assumption of electronic adiabaticity leads to the usual Born-Oppenheimer approximation, in which the electronic wave function is optimized for fixed nuclei. For solutes, the situation is more complicated because there are two types of heavy-body motion, the solute nuclear coordinates, which are treated mechanically, and the solvent, which is treated statistically. The SCRF procedures correspond to optimizing the electronic wave function in the presence of fixed solute nuclei and for a statistical distribution of solvent coordinates, which in turn are in equilibrium with the average electronic structure. The treatment of the solvent as a dielectric material by the laws of classical electrostatics and the treatment of the electronic charge distribution of the solute by the square of its wave function correctly embodies the result of

statistically averaging over a thermal solvent in equilibrium with an average (adiabatic) solute charge distribution. Because the self-consistent calculation of the adiabatic solute electronic distribution and the equilibrium polarization of the solvent is carried out at fixed solute atomic coordinates, the treatment corresponds most precisely to the case $\tau_s >> \tau_F >> \tau_{elec}$.

There are cases where the time scales do not satisfy these assumptions. Effects due to the violation of $\tau_s >> \tau_F$ are often called nonequilibrium solvation; and effects due to the violation of $\tau_F >> \tau_{elec}$ are often called nonadiabatic effects. The latter effects have been studied primarily in the context of electron transfer reactions. In electron transfer theory the interesting case of $\tau_{elec} >> \tau_F$ arises, and this is called nonadiabatic electron transfer. It occurs commonly for outer-sphere electron transfers in which ΔE_1 is very small in the critical configuration. For example ΔE_1 might be the energy difference of the symmetric and antisymmetric delocalized combinations of the two localized configurations $Fe^{3+}X_6 \cdots Fe^{2+}Y_6$ and $Fe^{2+}X_6 \cdots Fe^{3+}Y_6$, where X and Y are ligands, and $\cdots$ indicates only weak interaction between the ferrous and ferric centers. In contrast, for typical chemical reactions involving the making and/or breaking of bonds, as well as for many inner-sphere electron transfers ("inner-sphere" electron transfer refers to the case in which a ligand is part of the coordination sphere of both the donor and the acceptor), we have $\tau_F >> \tau_{elec}$, which is called the adiabatic case. For adiabatic electron transfers it is often assumed that $\tau_s >> \tau_F$ in which case the rate constant decreases as τ_F decreases. This regime is variously called high-friction [67], overdamped [333], or solvent-controlled adiabatic [356]. In adiabatic bond rearrangements (i.e., ordinary chemical reactions) on the other hand, one typically finds $\tau_F = \vartheta(\tau_s)$, in which case frictional effects are small but not necessarily completely negligible [357-359]; if $\tau_F > \tau_s$, this might be called bond-coordinate-controlled adiabatic. The other adiabatic case, $\tau_F >> \tau_s >> \tau_{elec}$ is called the low-friction [67], energy diffusion [333], or strong adiabatic [356] limit. In this case reaction is controlled by the rate of activation of reactants to the transition state, which is not in equilibrium with the reactants. The scenario just sketched leads to a pattern of the rate constant increasing with increasing friction at low friction, then becoming independent of friction, then decreasing as friction increases further [67]. This pattern can also be observed in the nonadiabatic case, but in that case the friction-independent region is wider [360]. When quantum mechanical effects are important, nonequilibrium effects may be very large [361]—this regime needs further study.

The SCRF models should be useful for any of the adiabatic cases, but a more quantitative treatment would recognize at least three time scales for frictional coupling based on the three times scales for dielectric polarization,

namely electronic, $\tau_{F,elec}$, vibrational, $\tau_{F,vib}$, and orientational, $\tau_{F,rot}$, with $\tau_{F,rot} >> \tau_{F,vib} >> \tau_{F,elec}$. The convenient adiabatic limit is never totally appropriate because $\tau_{F,elec} = \vartheta(\tau_{elec})$, even when $\tau_{F,vib} >> \tau_{elec}$.

One important phenomenon that sometimes occurs when $\tau_{elec} \geq \tau_F$ is solvent-induced charge localization. Thus, even though the adiabatic states are delocalized, the solvent-induced states are not. Consider the system $Fe^{3+}X_6 \cdots Fe^{2+}X_6$, which is the reactant of the outer-sphere electron transfer reaction mentioned above when X = Y. Clearly the ground state involves a symmetric linear combination of a state with the electron on the right (as written) and one with the electron on the left. Thus we could create the localized states by using the SCRF method to calculate the symmetric and antisymmetric stationary states and taking plus and minus linear combinations. This is reasonable but does not take account of the fact that the orbitals for non-transferred electrons should be optimized for the case where the transferred electron is localized (in contrast to which, the SCRF orbitals are all optimized for the delocalized adiabatic structure). The role of solvent-induced charge localization has also been studied for ionic dissociation reactions [109].

Having obtained the charge-localized state, the dynamics of electron transfer can be treated as a time-dependent configuration interaction problem [356, 362-364]. In this case the two configurations would be taken as the left localized and right localized ones. A more general treatment, applicable in the regime [365] where electronic coupling is larger (i.e., τ_{elec} is smaller), but electronic motion is still not adiabatic, would involve a 3-state CI composed of the delocalized adiabatic state interacting with the two localized diabatic ones.

In electron transfer reactions one studies the conversion of an electron state localized on A to one localized on B. One can also consider the relaxation of a charge localized state to the adiabatic delocalized state [366].

The most general available treatment of solute electronic structure that does not make the SCRF assumption that solvent electronic motion is slow compared to solute electronic motion is provided by the coherent-state formulation introduced by Kim and Hynes [109] and generalized by Bianco et al. [111]. Hynes and coworkers denote the SCRF limit simply as SC. They call the opposite limit [109, 173], in which the solvent polarization is fast compared to the vacuum solute electronic time scale, the Born-Oppenheimer (BO) limit, which should not be confused with the usual Born-Oppenheimer approximation for separating the electronic and nuclear motions of a gas-phase molecule or of the solute. Kim and Hynes note that one might also call this an adiabatic limit, which, they correctly note, would introduce other possible confusions. [Adiabatic and sudden limits have a long history of introducing confusion in many fields since

the opposite of an adiabatic limit is always another adiabatic limit. Consider for example, the case where x has a time scale that is rapid compared to the controlled, slow motion of y; then x adjusts almost adiabatically to that motion, and one can treat x by an adiabatic approximation or y by a sudden approximation. But the opposite limit, where x moves slowly compared to the timescale of y is also an adiabatic limit with y adjusting almost adiabatically to x, and x may be treated by a sudden approximation. Furthermore, even under the same conditions x may be sudden with respect to y, but adiabatic with respect to z. To avoid ambiguity one must be specific about which two variables are under consideration *and* which one is considered to be fast and adiabatic. This may, of course, be obvious from context, but often it is more obvious to the author than to the reader!]

The effective frequencies that characterize solvent response can be characterized more quantitatively from several points of view, including generalized Langevin theory [367-372], Brownian oscillators [373, 374], and instantaneous normal modes [375].

In addition to the intrinsic time scales of the system τ_F, τ_S, and τ_{elec}, one may introduce an additional time scale by the nature of the measurement. For example, electronic absorption spectroscopy may probe events on a time scale τ_{spect} that satisfies $\tau_{F,vib} >> \tau_{spect} >> \tau_{F,elec}$. In this case the excitation would occur to a state with the electronic contribution to solvation operative but the nuclear solvation coordinates frozen in their initial state. A direct analog would be gas-phase ultraviolet or visible spectroscopy with $\tau_S >> \tau_{spect} >> \tau_{elec}$. This leads to the familiar Franck-Condon principle [115] according to which the electronic state is changed but the nuclear motion is frozen during the excitation. In solution, this leads to the general observation that emission is red-shifted relative to absorption, since the orientational components of solvation are optimal only for the initial (in this case, excited-state) configuration.

Because of the economic importance of dyes, the calculation of solvent effects on electronic spectroscopy using the SCRF methods has been a subject of significant interest. The interesting dynamical issue that arises in this context is the fact that solute electronic excitation may be viewed as occurring essentially instantaneously on the solute reorientational time scale, as discussed in the preceding paragraph. We refer the reader to the original source literature for further details [167, 180, 181, 219, 298, 299, 376-380].

The reader is referred to review articles concerned with dynamic solvent effects for further discussion of the interesting issues involved in applying continuum and explicit solvation models to dynamical situations [333, 381-385].

6 Concluding remarks

There has been tremendous progress in the development and practical implementation of useful continuum solvation models in the last five years. These techniques are now poised to allow quantum chemistry to have the same revolutionary impact on condensed-phase chemistry as the last 25 years have witnessed for gas-phase chemistry.

7 Acknowledgments

This work was supported in part by the NSF and the U. S. Army Research Office.

References

1. A. Warshel and M. Levitt, *J. Mol. Biol.*, **103**, 227 (1976).
2. S. J. Weiner, U. C. Singh, and P. A. Kollman, *J. Am. Chem. Soc.*, **107**, 2219 (1985).
3. M. J. Field, P. A. Bash, and M. Karplus, *J. Comp. Chem.*, **11**, 700 (1990).
4. J. Gao, *J. Phys. Chem.*, **96**, 537 (1992).
5. V. V. Vasilyev, A. A. Bliznyuk, and A. A. Voityuk, *Int. J. Quant. Chem.*, **44**, 897 (1992).
6. R. V. Stanton, D. S. Hartsough, and K. M. Merz, *J. Phys. Chem.*, **97**, 11868 (1993).
7. V. Théry, D. Rinaldi, J.-L. Rivail, B. Maigret, and G. G. Ferenczy, *J. Comp. Chem.*, **15**, 269 (1994).
8. U. C. Singh and P. A. Kollman, *J. Comp. Chem.*, **7**, 718 (1986).
9. J. Gao, *J. Am. Chem. Soc.*, **115**, 2930 (1993).
10. J. L. Gao and X. F. Xia, *J. Am. Chem. Soc.*, **115**, 9667 (1993).
11. A. Warshel, T. Schewins, and M. Fothergill, *J. Am. Chem. Soc.*, **116**, 8437 (1994).
12. D. Wei and D. R. Salahub, *Chem. Phys. Lett.*, **224**, 291 (1994).
13. J. Gao, *J. Am. Chem. Soc.*, **116**, 1563 (1994).
14. J. Gao, *Proc Indian Acad. Sci. (Chem. Sci.)*, **106**, 507 (1994).
15. T. J. Marrone, D. S. Hartsough, and K. M. Merz, *J. Phys. Chem.*, **98**, 1341 (1994).
16. J. Gao, *J. Am. Chem. Soc.*, **116**, 9324 (1994).
17. J. Åqvist and A. Warshel, *Chem. Rev.*, **93**, 2418 (1993).
18. A. Warshel and Z. T. Chu, in *Structure and Reactivity in Aqueous Solution,* C. J. Cramer and D. G. Truhlar, Eds., American Chemical Society, Washington, DC, 1994 p. 71.
19. J. Gao, in *Reviews in Computational Chemistry,* K. B. Lipkowitz and D. B. Boyd, Eds., VCH, New York, Vol. 7, in press.
20. M. Sprik and M. L. Klein, *J. Chem. Phys.*, **89**, 7556 (1988).

21. U. Niesar, G. Corongiu, E. Clementi, G. R. Kneller, and D. K. Bhattacharya, *J. Chem. Phys.*, **94**, 7949 (1990).
22. L. X. Dang, J. E. Rice, J. Caldwell, and P. A. Kollman, *J. Am. Chem. Soc.*, **113**, 2481 (1991).
23. M. Sprik, *J. Chem. Phys.*, **95**, 6762 (1991).
24. L. X. Dang, *J. Chem. Phys.*, **97**, 2659 (1992).
25. S. W. Rick, S. J. Stuart, and B. J. Berne, *J. Chem. Phys.*, **101**, 6141 (1994).
26. S.-B. Zhu and C. F. Wong, *J. Phys. Chem.*, **98**, 4695 (1994).
27. I. Alkorta, M. Bachs, and J. J. Perez, *Chem. Phys. Lett.*, **224**, 160 (1994).
28. D. N. Bernardo, Y. Ding, K. Krogh-Jespersen, and R. M. Levy, *J. Phys. Chem.*, **98**, 4180 (1994).
29. D. Van Belle, M. Prévost, G. Kippens, and S. J. Wodak, in *Structure and Reactivity in Aqueous Solution,* C. J. Cramer and D. G. Truhlar, Eds., American Chemical Society, Washington, DC, 1994 p. 318.
30. L. S. Sremeniak, L. Perera, and M. L. Berkowitz, *Chem. Phys. Lett.*, **218**, 377 (1994).
31. D. A. McQuarrie, *Statistical Mechanics*. Harper & Row, New York, 1976.
32. H. Eyring, D. Henderson, D. J. Stover, and E. M. Eyring, *Statistical Mechanics and Dynamics*. John Wiley & Sons, New York, 1982.
33. M. P. Allen and D. J. Tildesley, *Computer Simulations of Liquids*. Oxford University Press, London, 1987.
34. J. A. McCammon and S. C. Harvey, *Dynamics of Proteins and Nucleic Acids*. Cambridge University Press, Cambridge, 1987.
35. D. L. Beveridge and F. M. DiCapua, *Annu. Rev. Biophys. Biophys. Chem.*, **18**, 431 (1989).
36. W. L. Jorgensen, *Acc. Chem. Res.*, **22**, 184 (1989).
37. P. M. King, C. A. Reynolds, J. W. Essex, G. A. Worth, and W. G. Richards, *Mol. Sim.*, **5**, 262 (1990).
38. D. W. Heermann, *Computer Simulation Methods in Theoretical Physics*. Springer-Verlag, Berlin, 1990.
39. K. Binder and D. W. Heermann, *Monte Carlo Simulation in Statistical Physics*. Springer-Verlag, Berlin, 1992.
40. P. Kollman, *Chem. Rev.*, **93**, 2395 (1993).
41. P. M. King, in *Computer Simulation of Biomolecular Systems,* W. F. van Gunsteren, P. K. Weinger and A. J. Wilkinson, Eds., ESCOM, Leiden, 1993, Vol. 2, p. 267.
42. W. F. van Gunsteren, F. J. Luque, D. Timms, and A. E. Torda, *Annu. Rev. Biophys. Biomol. Struct.*, **23**, 847 (1994).
43. J. Åqvist, C. Medina, and J.-E. Samuelsson, *Protein Eng.*, **7**, 385 (1994).
44. T. J. A. Ewing and T. P. Lybrand, *J. Phys. Chem.*, **98**, 1748 (1994).
45. D. A. Pearlman and P. A. Kollman, *J. Chem. Phys.*, **94**, 4532 (1991).
46. M. Mazor and B. M. Pettitt, *Mol. Sim.*, **6**, 1 (1991).

47. M. J. Mitchell and J. A. McCammon, *J. Comp. Chem.*, **12**, 271 (1991).
48. A. Hodel, T. Simonson, R. O. Fox, and A. T. Brünger, *J. Phys. Chem.*, **97**, 3409 (1993).
49. D. A. Pearlman, *J. Phys. Chem.*, **98**, 1487 (1994).
50. M. E. Clamp, P. G. Baker, C. J. Stirling, and A. Brass, *J. Comp. Chem.*, **15**, 838 (1994).
51. F. S. Lee and A. Warshel, *J. Chem. Phys.*, **97**, 3100 (1992).
52. K. Tasaki, S. McDonald, and J. W. Brady, *J. Comp. Chem.*, **14**, 278 (1993).
53. B. M. Ladanyi and M. S. Skaf, *Annu. Rev. Phys. Chem.*, **44**, 335 (1993).
54. P. J. Steinbach and B. R. Brooks, *J. Comp. Chem.*, **15**, 667 (1994).
55. J. W. Brady and R. K. Schmidt, *J. Phys. Chem.*, **97**, 958 (1993).
56. N. H. Frank and W. Tobocman, in *Fundamental Formulas of Physics,* D. H. Menzel, Ed. Dover, New York, 1960, Vol. 1, p. 307.
57. J. B. Marion, *Classical Electromagnetic Radiation.* Academic, New York, 1965.
58. K. Denbigh, *The Principles of Chemical Equilibrium.* Cambridge University Press, London, 1981.
59. M. Born, *Z. Physik*, **1**, 45 (1920).
60. L. Onsager, *Chem. Rev.*, **13**, 73 (1933).
61. J. G. Kirkwood, *J. Chem. Phys.*, **2**, 351 (1934).
62. J. G. Kirkwood, *J. Chem. Phys.*, **7**, 911 (1939).
63. B. Lee and F. M. Richards, *J. Mol. Biol.*, **55**, 379 (1971).
64. R. B. Hermann, *J. Phys. Chem.*, **76**, 2754 (1972).
65. M. G. Evans and M. Polanyi, *Trans. Faraday Soc.*, **31**, 875 (1935).
66. H. Eyring and W. F. K. Wynne-Jones, *J. Chem. Phys.*, **3**, 492 (1935).
67. M. M. Kreevoy and D. G. Truhlar, in *Investigation of Rates and Mechanisms of Reactions, Part I,* C. F. Bernasconi, Ed. Wiley, New York, 1986 p. 13.
68. H. A. Kramers, *Physica (The Hague)*, **7**, 284 (1940).
69. D. G. Truhlar, W. L. Hase, and J. T. Hynes, *J. Phys. Chem.*, **87**, 2664 (1983).
70. R. A. Marcus, *J. Chem. Phys.*, **24**, 979 (1956).
71. O. Tapia, in *Quantum Theory of Chemical Reactions,* R. Daudel, A. Pullman, L. Salem and A. Viellard, Eds., Reidel, Dordrecht, 1980, Vol. 2, p. 25.
72. O. Tapia, in *Molecular Interactions,* H. Rajaczak and W. J. Orville-Thomas, Eds., John Wiley & Sons, London, 1982, Vol. 3, p. 47.
73. M. L. J. Drummond, *Prog. Biophys. Mol. Biol.*, **47**, 1 (1986).
74. A. Rashin, *Int. J. Quant. Chem., Quant. Biol.*, **15**, 103 (1988).
75. M. E. Davis and J. A. McCammon, *Chem. Rev.*, **90**, 509 (1990).
76. J. Tomasi, R. Bonaccorsi, R. Cammi, and F. J. Olivares del Valle, *J. Mol. Struct. (Theochem)*, **234**, 401 (1991).
77. J. G. Ángyán, *J. Math. Chem.*, **10**, 93 (1992).
78. J. Tomasi, in *Structure and Reactivity in Aqueous Solution,* C. J. Cramer and D. G. Truhlar, Eds., American Chemical Society, Washington, DC, 1994 p. 10.
79. J. Tomasi and M. Persico, *Chem. Rev.*, **94**, 2027 (1994).

80. A. A. Rashin and M. A. Bukatin, *Biophys. Chem.*, **51**, 167 (1994).
81. C. J. Cramer and D. G. Truhlar, in *Quantitative Treatments of Solute/Solvent Interactions,* P. Politzer and J. S. Murray, Eds., Elsevier, Amsterdam, 1994, Vol. **1**, p. 9.
82. P. E. Smith and B. M. Pettitt, *J. Phys. Chem.*, **98**, 9700 (1994).
83. C. J. Cramer and D. G. Truhlar, in *Reviews in Computational Chemistry,* K. B. Lipkowitz and D. B. Boyd, Eds., VCH, New York, 1995, Vol. 6, p. 1.
84. W. K. H. Panofsky and M. Phillips, *Classical Electricity and Magnetism.* Addison-Wesley, Reading, MA, 1962.
85. D. R. Corson and P. Lorrain, *Introduction to Electromagnetic Fields and Waves.* W.H. Freeman, San Francisco, 1962.
86. J. E. Sanhueza, O. Tapia, W. G. Laidlaw, and M. Trsic, *J. Chem. Phys.*, **70**, 3096 (1979).
87. D. Rinaldi and J.-L. Rivail, *Theor. Chim. Acta*, **32**, 57 (1973).
88. J.-L. Rivail and D. Rinaldi, *Chem. Phys.*, **18**, 233 (1976).
89. S. Yomosa, *J. Phys. Soc. Japan*, **35**, 1738 (1973).
90. S. Yomosa, *J. Phys. Soc. Japan*, **36**, 1655 (1974).
91. O. Tapia and O. Goscinski, *Mol. Phys.*, **29**, 1653 (1975).
92. O. Tapia, E. Poulain, and F. Sussman, *Theor. Chim. Acta*, **47**, 171 (1978).
93. K. V. Mikkelsen, H. Agren, H. J. A. Jensen, and T. Helgaker, *J. Phys. Chem.*, **89**, 3086 (1988).
94. J.-L. Rivail, *Compt. Rend. Acad. Sci. Paris*, **311**, 307 (1990).
95. J.-L. Rivail, D. Rinaldi, and M. F. Ruiz-López, in *Theoretical and Computational Methods for Organic Chemistry,* S. J. Formosinho, I. G. Czismadia and L. G. Arnaut, Eds., Kluwer, Dordrecht, 1991 p. 79.
96. M. A. Aguilar, F. J. Olivares del Valle, and J. Tomasi, *J. Chem. Phys.*, **150**, 151 (1991).
97. F. J. Olivares del Valle and J. Tomasi, *Chem. Phys.*, **150**, 139 (1991).
98. F. J. Olivares del Valle, R. Bonaccorsi, R. Cammi, and J. Tomasi, *J. Mol. Struct. (Theochem)*, **230**, 295 (1991).
99. M. W. Wong, M. J. Frisch, and K. B. Wiberg, *J. Am. Chem. Soc.*, **113**, 4776 (1991).
100. C. Chipot, D. Rinaldi, and J.-L. Rivail, *Chem. Phys. Lett.*, **191**, 287 (1992).
101. F. J. Olivares del Valle and M. A. Aguilar, *J. Comp. Chem.*, **13**, 115 (1992).
102. J. G. Ángyán, *Int. J. Quant. Chem.*, **47**, 469 (1993).
103. F. J. Olivares del Valle and M. A. Aguilar, *J. Mol. Struct. (Theochem)*, **280**, 25 (1993).
104. F. J. Olivares del Valle, M. A. Aguilar, and S. Tolosa, *J. Mol. Struct. (Theochem)*, **279**, 223 (1993).
105. C. Chipot, L. G. Gorb, and J.-L. Rivail, *J. Phys. Chem.*, **98**, 1601 (1994).
106. K. V. Mikkelsen, P. Jørgensen, and H. J. A. Jensen, *J. Chem. Phys.*, **100**, 6597 (1994).

107. J. Jortner, *Mol. Phys.*, **5**, 257 (1962).
108. J. Gehlen, D. Chandler, H. J. Kim, and J. T. Hynes, *J. Phys. Chem.*, **96**, 1748 (1992).
109. H. J. Kim and J. T. Hynes, *J. Am. Chem. Soc.*, **114**, 10508 (1992).
110. M. V. Basilevsky, G. E. Chudinov, and M. D. Newton, *Chem. Phys.*, **179**, 263 (1994).
111. R. Bianco, J. J. I. Timoneda, and J. T. Hynes, *J. Phys. Chem.*, **98**, 12103 (1994).
112. O. Tapia, F. Colonna, and J. G. Angyan, *J. Chim. Phys.*, **87**, 875 (1990).
113. O. Tapia, *J. Mol. Struct. (Theochem)*, **226**, 59 (1991).
114. J. G. Ángyán, *J. Math. Chem.*, **10**, 93 (1992).
115. B. A. Bransden and C. J. Joachain, *Physics of Atoms and Molecules*. Longman, London, 1983.
116. C. J. F. Böttcher, O. C. van Belle, P. Bordewijk, and A. Rip, in *Theory of Electric Polarization*, Elsevier, Amsterdam, 1973 pp. 94ff.
117. O. Tapia and B. Silvi, *J. Phys. Chem.*, **84**, 2646 (1980).
118. P. Claverie, in *Quantum Theory of Chemical Reactions*, R. Daudel, A. Pullman, L. Salem and A. Veillard, Eds., Reidel, Dordrecht, 1982, Vol. 3, p. 151.
119. R. Constanciel and R. Contreras, *Theor. Chim. Acta*, **65**, 1 (1984).
120. E. L. Mehler, *Adv. Comput. Biol.*, **2**, in press (1995).
121. D. F. Eggers, N. W. Gregory, G. D. Halsey, and B. S. Rabinovitch, *Physical Chemistry*. John Wiley & Sons, New York, 1964.
122. B. J. Yoon and A. M. Lenhoff, *J. Comp. Chem.*, **11**, 1080 (1990).
123. V. Frecer and S. Miertus, *Int. J. Quant. Chem.*, **42**, 1449 (1992).
124. G. G. Hammes, *Principles of Chemical Kinetics*. Academic, New York, 1977.
125. M. Holst, R. E. Kozack, F. Saied, and S. Subramanian, *J. Biomol. Struct. Dynam.*, **11**, 1437 (1994).
126. S. P. Slagle, R. E. Kozack, and S. Subramanian, *J. Biomol. Struct. Dynam.*, **12**, 439 (1994).
127. P. Debye, *Polar Molecules*. Chemical Catalog Co., New York, 1929.
128. B. Roux, H.-A. Yu, and M. Karplus, *J. Phys. Chem.*, **94**, 4683 (1990).
129. F. Figueirido, G. S. Del Buono, and R. M. Levy, *Biophys. Chem.*, **51**, 235 (1994).
130. M. Bucher and T. L. Porter, *J. Phys. Chem.*, **90**, 3406 (1986).
131. S. Ehrenson, *J. Comp. Chem.*, **10**, 77 (1989).
132. A. Wallqvist, *Chem. Phys. Lett.*, **165**, 437 (1990).
133. N. Matubayasi, L. H. Reed, and R. M. Levy, *J. Phys. Chem.*, **98**, 10640 (1994).
134. A. A. Rashin and M. A. Bukatin, *J. Phys. Chem.*, **98**, 386 (1994).
135. P. Jungwirth and R. Zahradnik, *Chem. Phys. Lett.*, **217**, 319 (1994).
136. T. Lazaridis and M. E. Paulaitis, *J. Phys. Chem.*, **98**, 635 (1994).
137. I. I. Vaisman, F. K. Brown, and A. Tropsha, *J. Phys. Chem.*, **98**, 5559 (1994).
138. I. Tuñón, E. Silla, and J. L. Pascual-Ahuir, *Protein Eng.*, **5**, 715 (1992).
139. R. M. Lynden-Bell, *J. Phys. Chem.*, **97**, 2991 (1993).
140. H. S. Chan and K. A. Dill, *J. Chem. Phys.*, **101**, 7007 (1994).

141. D. J. Giesen, C. J. Cramer, and D. G. Truhlar, *J. Phys. Chem.*, **98**, 4141 (1994).
142. R. A. Pierotti, *J. Phys. Chem.*, **67**, 1840 (1963).
143. B. Linder, *Adv. Chem. Phys.*, **12**, 225 (1967).
144. H. Hoshi, M. Sakurai, Y. Inouye, and R. Chûjô, *J. Chem. Phys.*, **87**, 1107 (1987).
145. R. Bonaccorsi, E. Ojalvo, and J. Tomasi, *Coll. Czech. Chem. Comm.*, **53**, 2320 (1988).
146. R. Bonaccorsi, F. Floris, P. Palla, and J. Tomasi, *Theor. Chim. Acta*, **162**, 213 (1990).
147. R. Bonaccorsi, E. Ojalvo, P. Palla, and J. Tomasi, *Chem. Phys.*, **143**, 245 (1990).
148. M. Cossi, B. Mennucci, and J. Tomasi, *Chem. Phys. Lett.*, **228**, 165 (1994).
149. K. A. Sharp and B. Honig, *Annu. Rev. Biophys. Biophys. Chem.*, **19**, 301 (1990).
150. K. Sharp, A. Jean-Charles, and B. Honig, *J. Phys. Chem.*, **96**, 3822 (1992).
151. D. Sitkoff, K. A. Sharp, and B. Honig, *J. Phys. Chem.*, **98**, 1978 (1994).
152. A. Rashin, *J. Phys. Chem.*, **94**, 1725 (1990).
153. V. Mohan, M. E. Davis, J. A. McCammon, and B. M. Pettitt, *J. Phys. Chem.*, **96**, 6428 (1992).
154. C. Lim, S. L. Chan, and P. Tole, in *Structure and Reactivity in Aqueous Solution*, C. J. Cramer and D. G. Truhlar, Eds., American Chemical Society, Washington, DC, 1994, Vol. 568, p. 50.
155. L. Onsager, *J. Am. Chem. Soc.*, **58**, 1486 (1936).
156. A. Dega-Szafran, M. Gdaniec, M. Grunwald-Wyspianska, Z. Kosturkiewicz, J. Koput, P. Krzyzanowski, and M. Szafran, *J. Mol. Struct.*, **270**, 99 (1992).
157. M. Szafran, M. M. Karelson, A. R. Katritzky, J. Koput, and M. C. Zerner, *J. Comp. Chem.*, **14**, 371 (1993).
158. M. W. Wong, K. B. Wiberg, and M. J. Frisch, *J. Chem. Phys.*, **95**, 8991 (1991).
159. L. C. G. Freitas, R. L. Longo, and A. M. Simas, *J. Chem. Soc., Faraday Trans.*, **88**, 189 (1992).
160. C. Adamo and F. Lelj, *Chem. Phys. Lett.*, **223**, 54 (1994).
161. S. C. Tucker and D. G. Truhlar, *Chem. Phys. Lett.*, **157**, 164 (1989).
162. J. L. Rivail and B. Terryn, *J. Chem. Phys.*, **79**, 1 (1982).
163. D. Rinaldi, M. F. Ruiz-Lopez, and J.-L. Rivail, *J. Chem. Phys.*, **78**, 834 (1983).
164. V. Dillet, D. Rinaldi, J. G. Angyán, and J.-L. Rivail, *Chem. Phys. Lett.*, **202**, 18 (1993).
165. V. Dillet, D. Rinaldi, and J.-L. Rivail, *J. Phys. Chem.*, **98**, 5034 (1994).
166. G. P. Ford and B. Wang, *J. Comp. Chem.*, **13**, 229 (1992).
167. R. R. Pappalardo, M. Reguero, and M. A. Robb, *Chem. Phys. Lett.*, **212**, 12 (1993).
168. M. J. Huron and P. Claverie, *J. Phys. Chem.*, **76**, 2123 (1972).
169. H. L. Friedman, *Mol. Phys.*, **29**, 29 (1975).
170. J. I. Gersten and A. M. Sapse, *J. Am. Chem. Soc.*, **107**, 3786 (1985).
171. G. Karlström, *J. Phys. Chem.*, **92**, 1315 (1988).
172. M. Karelson, T. Tamm, and M. C. Zerner, *J. Phys. Chem.*, **97**, 11901 (1993).

173. H. J. Kim, R. Bianco, B. J. Gertner, and J. T. Hynes, *J. Phys. Chem.*, **97**, 1723 (1993).
174. J. T. Hynes, H. J. Kim, J. R. Mathis, and J. Juanos i Timoneda, *J. Mol. Liquids*, **57**, 53 (1993).
175. S. Miertus, E. Scrocco, and J. Tomasi, *Chem. Phys.*, **55**, 117 (1981).
176. H. Hoshi, M. Sakurai, Y. Inoue, and R. Chûjô, *J. Mol. Struct. (Theochem)*, **180**, 267 (1988).
177. T. Furuki, A. Umeda, M. Sakurai, Y. Inoue, and R. Chûjô, *J. Comp. Chem.*, **15**, 90 (1994).
178. G. P. Ford and B. Wang, *J. Am. Chem. Soc.*, **114**, 10563 (1992).
179. B. Wang and G. P. Ford, *J. Chem. Phys.*, **97**, 4162 (1992).
180. T. Fox and N. Rosch, *J. Mol. Struct. (Theochem)*, **276**, 279 (1992).
181. T. Fox, N. Rösch, and R. J. Zauhar, *J. Comp. Chem.*, **14**, 253 (1993).
182. M. Negre, M. Orozco, and F. J. Luque, *Chem. Phys. Lett.*, **196**, 27 (1992).
183. F. J. Luque, M. J. Negre, and M. Orozco, *J. Phys. Chem.*, **97**, 4386 (1993).
184. A. A. Rashin, M. A. Bukatin, J. Andzelm, and A. T. Hagler, *Biophys. Chem.*, **51**, 375 (1994).
185. K. Baldridge, R. Fine, and A. Hagler, *J. Comp. Chem.*, **15**, 1217 (1994).
186. Y. Chen, L. Noodleman, D. A. Case, and D. Bashford, *J. Phys. Chem.*, **98**, 11059 (1994).
187. F. Peradejordi, *Cahiers Phys.*, **17**, 343 (1963).
188. T. Kozaki, K. Morihashi, and O. Kikuchi, *J. Mol. Struct. (Theochem)*, **168**, 265 (1988).
189. T. Kozaki, M. Morihashi, and O. Kikuchi, *J. Am. Chem. Soc.*, **111**, 1547 (1989).
190. A. Klamt and G. Schüürmann, *J. Chem. Soc., Perkin Trans.* 2, 799 (1993).
191. D. Eisenberg and A. D. McLachlan, *Nature*, **319**, 199 (1986).
192. T. Ooi, M. Oobatake, G. Nemethy, and H. A. Scheraga, *Proc. Natl. Acad. Sci., USA*, **84**, 3086 (1987).
193. W. C. Still, A. Tempczyk, R. C. Hawley, and T. Hendrickson, *J. Am. Chem. Soc.*, **112**, 6127 (1990).
194. D. Rinaldi, B. J. Costa Cabral, and J.-L. Rivail, *Chem. Phys. Lett.*, **125**, 495 (1986).
195. P. Young, D. V. S. Green, I. H. Hillier, and N. A. Burton, *Mol. Phys.*, **80**, 503 (1993).
196. I. Tuñón, E. Silla, and J. Bertrán, *J. Phys. Chem.*, **97**, 5547 (1993).
197. J. Langlet, P. Claverie, J. Caillet, and A. Pullman, *J. Phys. Chem.*, **92**, 1617 (1988).
198. H. Sato and S. Kato, *J. Mol. Struct. (Theochem)*, **310**, 67 (1994).
199. E. O. Purisima and S. H. Nilar, *J. Comp. Chem.*, **16**, 681 (1995).
200. A. Varnek, G. Wipff, A. S. Glebov, and D. Feil, *J. Comp. Chem.*, **16**, 1 (1995).
201. G. Karlström and B. Halle, *J. Chem. Phys.*, **99**, 8056 (1993).
202. F. Floris and J. Tomasi, *J. Comp. Chem.*, **10**, 616 (1989).
203. F. M. Floris, J. Tomasi, and J. L. Pascual-Ahuir, *J. Comp. Chem.*, **39**, 784 (1991).
204. C. Amovilli, *Chem. Phys. Lett.*, **229**, 244 (1994).

205. M. Bachs, F. J. Luque, and M. Orozco, *J. Comp. Chem.*, **15**, 446 (1994).
206. F. J. Luque, M. Bachs, and M. Orozco, *J. Comp. Chem.*, **15**, 847 (1994).
207. M. Orozco, M. Bachs, and F. J. Luque, *J. Comp. Chem.*, **16**, 563 (1995).
208. F. J. Luque, C. Alemán, M. Bachs, and M. Orozco, preprint
209. F. J. Luque, C. Alemán, and M. Orozco, preprint
210. C. J. Cramer and D. G. Truhlar, *J. Am. Chem. Soc.*, **113**, 8305 (1991).
211. C. J. Cramer and D. G. Truhlar, *Science*, **256**, 213 (1992).
212. C. J. Cramer and D. G. Truhlar, *J. Comp. Chem.*, **13**, 1089 (1992).
213. J. W. Storer, D. J. Giesen, G. D. Hawkins, G. C. Lynch, C. J. Cramer, D. G. Truhlar, and D. A. Liotard, in *Structure and Reactivity in Aqueous Solution,* C. J. Cramer and D. G. Truhlar, Eds., American Chemical Society, Washington, DC, 1994 p. 24.
214. D. A. Liotard, G. D. Hawkins, G. C. Lynch, C. J. Cramer, and D. G. Truhlar, *J. Comp. Chem.*, **16**, 422 (1995).
215. G. D. Hawkins, C. J. Cramer, and D. G. Truhlar, *Chem. Phys. Lett.*, submitted for publication
216. D. J. Giesen, J. W. Storer, C. J. Cramer, and D. G. Truhlar, *J. Am. Chem. Soc.*, **117**, 1057 (1995).
217. D. J. Giesen, C. J. Cramer, and D. G. Truhlar, *J. Phys. Chem.*, **99**, 7137 (1995).
218. C. C. Chambers, D. J. Giesen, C. J. Cramer, and D. G. Truhlar, to be published
219. G. Rauhut, T. Clark, and T. Steinke, *J. Am. Chem. Soc.*, **115**, 9174 (1993).
220. D. J. Tannor, B. Marten, R. Murphy, R. A. Friesner, D. Sitkoff, A. Nicholls, M. Ringnalda, W. A. Goddard, and B. Honig, *J. Am. Chem. Soc.*, **116**, 11875 (1994).
221. R. W. Dixon, J. M. Leonard, and W. J. Hehre, *Israel J. Chem.*, **33**, 427 (1993).
222. T. N. Truong and E. V. Stefanovich, *Chem. Phys. Lett.*, **240**, 253 (1995).
223. T. N. Truong and E. V. Stefanovich, *J. Chem. Phys.*, in press.
224. D. Thirumalai, K. Onda, and D. G. Truhlar, *J. Chem. Phys.*, **74**, 526 (1981).
225. A. J. Stone, *Chem. Phys. Lett.*, **83**, 233 (1981).
226. A. J. Stone and M. Alderton, *Mol. Phys.*, **56**, 1047 (1985).
227. W. A. Sokalski, D. A. Keller, R. L. Ornstein, and R. Rein, *J. Comp. Chem.*, **14**, 970 (1993).
228. C. Chipot, J. G. Angyán, G. G. Ferenczy, and H. A. Scheraga, *J. Phys. Chem.*, **97**, 6628 (1993).
229. D. E. Williams, *J. Comp. Chem.*, **15**, 719 (1994).
230. G. J. Hoijtink, E. de Boer, P. H. Van der Meij, and W. P. Weijland, *Recl. Trav. Chim. Pays-Bas*, **75**, 487 (1956).
231. I. Jano, *Compt. Rend. Acad. Sci. Paris*, **261**, 103 (1965).
232. G. Klopman, *Chem. Phys. Lett.*, **1**, 200 (1967).
233. R. Contreras and A. Aizman, *Int. J. Quant. Chem.*, **27**, 293 (1985).
234. M. Schaefer and C. Froemmel, *J. Mol. Biol.*, **216**, 1045 (1990).
235. J. W. Storer, D. J. Giesen, C. J. Cramer, and D. G. Truhlar, *J. Comput.-Aid. Mol. Des.*, **9**, 87 (1995).

236. C. J. Cramer and D. G. Truhlar, *J. Comput.-Aid. Mol. Des.*, **6**, 629 (1992).
237. I. Alkorta, H. O. Villar, and J. J. Perez, *J. Comp. Chem.*, **14**, 620 (1993).
238. C. J. Cramer, G. D. Hawkins, and D. G. Truhlar, *J. Chem. Soc., Faraday Trans.*, **90**, 1802 (1994).
239. A. Ben-Naim, *Statistical Thermodynamics for Chemists and Biochemists*. Plenum, New York, 1992.
240. C. Reichardt, *Solvents and Solvent Effects in Organic Chemistry*. VCH, New York, 1990.
241. L. Streyer, *Biochemistry*. W. H. Freeman and Co., New York, 1981.
242. K. Ijima, K. Tanaka, and S. Onuma, *J. Mol. Struct.*, **246**, 257 (1991).
243. R. Bonaccorsi, P. Palla, and J. Tomasi, *J. Am. Chem. Soc.*, **106**, 1945 (1984).
244. J. S. Gaffney, R. C. Pierce, and L. Friedman, *J. Am. Chem. Soc.*, **99**, 4293 (1977).
245. W. J. Hehre, L. Radom, P. v. R. Schleyer, and J. A. Pople, *Ab Initio Molecular Orbital Theory*. Wiley, New York, 1986.
246. W. J. Hehre, L. D. Burke, A. J. Shusterman, and W. J. Pietro, *Experiments in Computational Organic Chemistry*. Wavefunction Inc., Irvine, CA, 1993.
247. W. J. Pietro, *J. Chem. Ed.*, **71**, 416 (1994).
248. S. Inouye, *Chem. Pharm. Bull.*, **16**, 1134 (1968).
249. W. C. Herndon, *J. Phys. Org. Chem.*, **6**, 634 (1993).
250. S. H. Hilal, L. A. Carreira, G. L. Baughman, S. W. Karickhoff, and C. M. Melton, *J. Phys. Org. Chem.*, **7**, 122 (1994).
251. E. Rajasekaran, B. Jayaram, and B. Honig, *J. Am. Chem. Soc.*, **116**, 8238 (1994).
252. J. J. Urban, R. L. Vontersch, and G. R. Famini, *J. Org. Chem.*, **59**, 5239 (1994).
253. B. Terryn, J.-L. Rivail, and D. Rinaldi, *J. Chem. Res. (S)*, 141 (1981).
254. S. Galera, A. Oliva, J. M. Lluch, and J. Bertrán, *J. Mol. Struct. (Theochem)*, **110**, 15 (1984).
255. J. L. Pascual-Ahuir, J. Andres, and E. Silla, *Chem. Phys. Lett.*, **169**, 297 (1990).
256. I. Tuñón, E. Silla, and J. Tomas, *J. Phys. Chem.*, **96**, 9043 (1992).
257. D. H. Aue, H. M. Webb, and M. T. Bowers, *J. Am. Chem. Soc.*, **98**, 311 (1976).
258. M. Meot-Ner and L. W. Sieck, *J. Am. Chem. Soc.*, **113**, 4448 (1991).
259. R. C. Weast, Ed., *CRC Handbook of Chemistry and Physics* CRC Press, Boca Raton, FL, 1980.
260. C. J. Cramer and D. G. Truhlar, *J. Am. Chem. Soc.*, **113**, 8552 9901(E) (1991).
261. I. Tuñón, E. Silla, and J.-L. Pascual-Ahuir, *J. Am. Chem. Soc.*, **115**, 2226 (1993).
262. J.-L. Rivail, S. Antoczak, C. Chipot, M. F. Ruiz-López, and L. G. Gorb, in *Structure and Reactivity in Aqueous Solution*, C. J. Cramer and D. G. Truhlar, Eds., American Chemical Society, Washington, DC, 1994, Vol. 568, p. 154.
263. K. Ando and J. T. Hynes, in *Structure and Reactivity in Aqueous Solution*, C. J. Cramer and D. G. Truhlar, Eds., American Chemical Society, Washington, DC, 1994, Vol. 568, p. 143.
264. R. A. Marcus, *Annu. Rev. Phys. Chem.*, **15**, 155 (1964).
265. R. A. Robertson, *Trans. Faraday Soc.*, **32**, 743 (1936).

266. A. R. Katritzky, *Handbook of Heterocyclic Chemistry*. Pergamon, Oxford, 1985.
267. J. S. Kwiatkowski, T. J. Zielinski, and R. Rein, *Adv. Quantum Chem.*, **18**, 85 (1986).
268. M. M. Karelson, A. R. Katritzky, M. Szafran, and M. C. Zerner, *J. Chem. Soc., Perkin Trans. 2*, 195 (1990).
269. M. M. Karelson, T. Tamm, A. R. Katritzky, S. J. Cato, and M. C. Zerner, *Tetrahedron Comput. Methodol.*, **2**, 295 (1989).
270. H. S. Rzepa, M. Y. Yi, M. M. Karelson, and M. C. Zerner, *J. Chem. Soc., Perkin Trans. 2*, 635 (1991).
271. O. G. Parchment, D. V. S. Green, P. J. Taylor, and I. H. Hillier, *J. Am. Chem. Soc.*, **115**, 2352 (1993).
272. S. Woodcock, D. V. S. Green, M. A. Vincent, I. H. Hillier, M. F. Guest, and P. Sherwood, *J. Chem. Soc., Perkin Trans. 2*, 2151 (1992).
273. M. A. Aguilar and F. J. Olivares del Valle, *Chem. Phys.*, **129**, 439 (1989).
274. U. C. Singh and P. A. Kollman, *J. Comp. Chem.*, **5**, 129 (1984).
275. W. L. Jorgensen, J. Chandrasekhar, J. D. Madura, R. W. Impey, and M. L. Klein, *J. Chem. Phys.*, **79**, 926 (1983).
276. S. J. Weiner, P. A. Kollman, D. T. Nguyen, and D. A. Case, *J. Comp. Chem.*, **7**, 230 (1986).
277. C. J. Cramer and D. G. Truhlar, *J. Am. Chem. Soc.*, **115**, 8810 (1993).
278. A. R. Katritzky and J. M. Lagowski, *Adv. Heterocycl. Chem.*, **6**, 1 (1963).
279. J. Elguero, C. Marzin, A. R. Katritzky, and P. Linda, *The Tautomerism of Heterocycles*. Academic, New York, 1976.
280. I. R. Gould and I. H. Hillier, *J. Chem. Soc., Perkin Trans. 2*, 1771 (1993).
281. F. Tomás, J. Catalán, P. Pérez, and J. Elguero, *J. Org. Chem.*, **59**, 2799 (1994).
282. J. Catalán, P. Pérez, and J. Elguero, *J. Org. Chem.*, **58**, 5276 (1993).
283. D. S. Wofford, D. M. Forkey, and J. G. Russell, *J. Org. Chem.*, **47**, 5132 (1982).
284. W. M. F. Fabian, *J. Comp. Chem.*, **12**, 17 (1991).
285. O. G. Parchment, I. H. Hillier, D. V. S. Green, N. A. Burton, J. O. Morley, and H. F. Schaefer, *J. Chem. Soc., Perkin Trans. 2*, 1681 (1992).
286. H. Fritz, *Bull. Soc. Chim. Belg.*, **93**, 559 (1984).
287. M. W. Wong, R. Leung-Toung, and C. Wentrup, *J. Am. Chem. Soc.*, **115**, 2465 (1993).
288. P. Beak, *Acc. Chem. Res.*, **10**, 186 (1977).
289. L. D. Hatherley, R. D. Brown, P. D. Godfrey, A. P. Pierlot, W. Caminati, D. Damiani, S. Melandri, and L. B. Favero, *J. Phys. Chem.*, **97**, 46 (1993).
290. A. Les, L. Adamowicz, M. J. Nowak, and L. Lapinski, *J. Mol. Struct. (Theochem)*, **277**, 313 (1992).
291. O. G. Parchment, N. A. Burton, and I. H. Hillier, *Chem. Phys. Lett.*, **203**, 46 (1993).
292. R. J. Hall, N. A. Burton, I. H. Hillier, and P. E. Young, *Chem. Phys. Lett.*, **220**, 129 (1994).
293. V. Barone and C. Adamo, *Chem. Phys. Lett.*, **226**, 399 (1994).

294. J. S. Kwiatkowski and A. Tempczyk, *Chem. Phys.*, **85**, 397 (1984).
295. M. M. Karelson, A. R. Katritzky, M. Szafran, and M. C. Zerner, *J. Org. Chem.*, **54**, 6030 (1989).
296. H. S. Rzepa and M. Y. Yi, *J. Chem. Soc., Perkin Trans. 2*, 531 (1991).
297. M. W. Wong, K. B. Wiberg, and M. J. Frisch, *J. Am. Chem. Soc.*, **114**, 1645 (1992).
298. V. Barone and C. Adamo, *J. Comp. Chem.*, **15**, 395 (1994).
299. V. Barone and C. Adamo, *J. Photochem. Photobiol. A: Chem.*, **80**, 211 (1994).
300. J. E. Del Bene, *J. Phys. Chem.*, **98**, 5902 (1994).
301. B. Wang and G. P. Ford, personal communication.
302. S. H. Vosko, L. Wilks, and M. Nussair, *Can. J. Phys.*, **58**, 1200 (1980).
303. A. D. Becke, *Phys. Rev. A*, **38**, 3098 (1988).
304. J. P. Perdew, *Physical Reviews B*, **33**, 8822 (1986).
305. P. O. Löwdin, *Adv. Quantum Chem.*, **2**, 213 (1965).
306. B. Pullman and A. Pullman, *Adv. Heterocycl. Chem.*, **13**, 77 (1971).
307. M. D. Topal and J. R. Fresco, *Nature*, **263**, 285 (1976).
308. M. Szczeniak, K. Szczepaniak, J. S. Kwiatkowski, K. KuBulat, and W. B. Person, *J. Am. Chem. Soc.*, **110**, 8319 (1988).
309. M. Scanlan and I. H. Hillier, *J. Am. Chem. Soc.*, **106**, 3737 (1984).
310. J. S. Kwiatkowski, R. J. Bartlett, and W. B. Person, *J. Am. Chem. Soc.*, **110**, 2353 (1988).
311. A. Les, L. Adamowicz, and R. J. Bartlett, *J. Phys. Chem.*, **93**, 4001 (1989).
312. J. Leszcynski, *J. Phys. Chem.*, **96**, 1649 (1992).
313. J. W. Boughton and P. Pulay, *Int. J. Quant. Chem.*, **47**, 49 (1993).
314. D. A. Estrin, L. Paglieri, and G. Corongiu, *J. Phys. Chem.*, **98**, 5653 (1994).
315. A. R. Katritzky and M. Karelson, *J. Am. Chem. Soc.*, **113**, 1561 (1991).
316. P. E. Young and I. H. Hillier, *Chem. Phys. Lett.*, **215**, 405 (1993).
317. M. Orozco and F. J. Luque, *J. Am. Chem. Soc.*, **117**, 1378 (1995).
318. J. G. Contreras and J. B. Alderete, *J. Mol. Struct. (Theochem)*, **309**, 137 (1994).
319. C. Alhambra, F. J. Luque, J. Estelrich, and M. Orozco, *J. Org. Chem.*, **60**, 969 (1995).
320. J. G. Contreras and J. B. Alderte, *Bol. Sci. Chil. Quim.*, **39**, 17 (1994).
321. J. G. Contreras and J. B. Alderete, *Chem. Phys. Lett.*, **232**, 61 (1995).
322. X.-C. Wang, J. Nichols, M. Feyereisen, M. Gutowski, J. Boatz, A. D. J. Haymet, and J. Simons, *J. Phys. Chem.*, **95**, 10419 (1991).
323. G. Briegleb and W. Strohmeier, *Angew. Chem.*, **64**, 409 (1952).
324. S. G. Mills and P. Beak, *J. Org. Chem.*, **50**, 1216 (1985).
325. S. E. Barrows, F. J. Dulles, C. J. Cramer, D. G. Truhlar, and A. D. French, *Carbohydr. Res.*, in press
326. H. B. Broughton and P. R. Woodward, *J. Comput.-Aid. Mol. Des.*, **4**, 147 (1990).
327. S. Gelin and P. Pollet, *Tetrahedron Lett.*, **21**, 4491 (1980).
328. K. Saito and T. Yamaguchi, *J. Chem. Soc., Perkin Trans. 2*, 1605 (1979).

329. J. Whiting and J. T. Edward, *Can. J. Chem.*, **49**, 3799 (1971).
330. D. Chandler and L. R. Pratt, *J. Chem. Phys.*, **65**, 2925 (1976).
331. L. R. Pratt and D. C. Chandler, *J. Chem. Phys.*, **67**, 3683 (1977).
332. D. Chandler, *J. Chem. Phys.*, **68**, 2959 (1978).
333. J. T. Hynes, in *Theory of Chemical Reaction Dynamics,* M. Baer, Ed. CRC Press, Boca Raton, 1985, Vol. 4, p. 171.
334. T. L. Hill, *Statistical Mechanics: Principles and Selected Applications.* McGraw-Hill, New York, 1956.
335. D. J. Tobias, S. F. Sneddon, and C. L. Brooks, *J. Mol. Biol.*, **216**, 783 (1990).
336. G. J. Tawa and L. R. Pratt, in *Structure and Reactivity in Aqueous Solution,* C. J. Cramer and D. G. Truhlar, Eds., American Chemical Society, Washington, DC, 1994, Vol. 568, p. 60.
337. T. C. Beutler and W. F. van Gunsteren, *Chem. Phys. Lett.*, **237**, 308 (1995).
338. C. Ritchie, *Pure Appl. Chem.*, **51**, 153 (1979).
339. J. Jaume, J. M. Lluch, A. Oliva, and J. Bertrán, *Chem. Phys. Lett.*, **106**, 232 (1984).
340. S. C. Tucker and D. G. Truhlar, *J. Am. Chem. Soc.*, **112**, 3347 (1990).
341. C. J. Cramer and D. G. Truhlar, *J. Am. Chem. Soc.*, **114**, 8794 (1992).
342. I. Tuñón, E. Silla, and J. Bertrán, *J. Chem. Soc., Faraday Trans.*, **90**, 1757 (1994).
343. J. Frau, J. Donoso, F. Muñoz, and F. G. Blanco, *Helv. Chim. Acta*, **77**, 1557 (1994).
344. J. Bertrán, J. M. Lluch, A. Gonzalez-Lafont, V. Dillet, and V. Pérez, in *Structure and Reactivity in Aqueous Solution,* C. J. Cramer and D. G. Truhlar, Eds., American Chemical Society, Washington, DC, 1994, Vol. 568, p. 168.
345. P. M. Morse, *Thermal Physics.* W. A. Benjamin, New York, 1969.
346. C. V. Heer, *Statistical Mechanics, Kinetic Theory, and Stochastic Processes.* Academic, New York, 1972.
347. J. McConnell, *Rotational Brownian Motion and Dielectric Theory.* Academic, New York, 1980.
348. L. D. Zusman, *Soviet Phys. JETP*, **42**, 794 (1976).
349. I. Rips and J. Jortner, *J. Chem. Phys.*, **87**, 2090 (1987).
350. J. Hubbard and L. Onsager, *J. Chem. Phys.*, **67**, 4850 (1977).
351. D. Kivelson and H. Friedman, *J. Chem. Phys.*, **93**, 7026 (1989).
352. R. Saxton, *Proc. R. Soc. London*, **A213**, 473 (1952).
353. S. K. Garg and C. P. Smyth, *J. Phys. Chem.*, **69**, 1294 (1965).
354. J. Crossley, *Adv. Molec. Relax. Processes*, **2**, 69 (1970).
355. L. D. Zusman, *Chem. Phys.*, **119**, 51 (1988).
356. Z. Wang, J. Tang, and J. R. Norris, *J. Chem. Phys.*, **97**, 7251 (1992).
357. S. Lee and J. T. Hynes, *J. Chem. Phys.*, **88**, 6863 (1988).
358. M. V. Basilevsky, G. E. Chudinov, and D. W. Napolov, *J. Phys. Chem.*, **97**, 3270 (1993).
359. D. G. Truhlar, G. K. Schenter, and B. C. Garrett, *J. Chem. Phys.*, **98**, 5756 (1993).
360. A. I. Burshtein and A. A. Zharikov, *Chem. Phys.*, **152**, 23 (1956).

361. B. C. Garrett and G. K. Schenter, in *Structure and Reactivity in Aqueous Solution,* C. J. Cramer and D. G. Truhlar, Eds., American Chemical Society, Washington, DC, 1994, Vol. 568, p. 122.
362. L. D. Zusman, *Chem. Phys.*, **49**, 265 (1980).
363. A. Garg, J. N. Onuchic, and V. Ambegaokar, *J. Chem. Phys.*, **83**, 4491 (1985).
364. M. V. Basilevsky and G. E. Chudinov, *Chem. Phys.*, **157**, 345 (1991).
365. H. J. Kim and J. T. Hynes, *J. Chem. Phys.*, **93**, 5211 (1990).
366. I. V. Alexandrov, *Chem. Phys.*, **51**, 449 (1980).
367. R. Zwanzig, *J. Stat. Phys.*, **9**, 215 (1973).
368. S. A. Adelman and J. D. Dull, *J. Chem. Phys.*, **64**, 2375 (1976).
369. S. A. Adelman, *Adv. Chem. Phys.*, **44**, 143 (1980).
370. S. A. Adelman and C. L. Brooks, *J. Phys. Chem.*, **86**, 1511 (1982).
371. R. F. Grote and J. T. Hynes, *J. Chem. Phys.*, **73**, 2715 (1980).
372. G. van der Zwan and J. T. Hynes, *J. Chem. Phys.*, **78**, 4174 (1983).
373. S. Mukamel, *Annu. Rev. Phys. Chem.*, **41**, 647 (1990).
374. L. E. Fried and S. Mukamel, *Adv. Chem. Phys.*, **84**, 435 (1993).
375. R. M. Stratt, *Acc. Chem. Res.*, **28**, 201 (1995).
376. M. Karelson and M. C. Zerner, *J. Am. Chem. Soc.*, **112**, 9405 (1990).
377. M. M. Karelson and M. C. Zerner, *J. Phys. Chem.*, **96**, 6949 (1992).
378. T. Fox and N. Rösch, *Chem. Phys. Lett.*, **191**, 33 (1992).
379. N. Rösch and M. C. Zerner, *J. Phys. Chem.*, **98**, 5817 (1994).
380. A. Klamt, preprint
381. D. Chandler, in *Liquids, Freezing, and Glass Transition,* J. P. Hansen, D. Levesque and J. Zinn-Justin, Eds., Elsevier, Amsterdam, 1991 p. 193.
382. M. J. Weaver, *Chem. Rev.*, **92**, 463 (1992).
383. B. C. Garrett and G. K. Schenter, *Int. Rev. Phys. Chem.*, **13**, 263 (1994).
384. P. J. Rossky and J. D. Simon, *Nature*, **370**, 263 (1994).
385. S. C. Tucker, in *New Trends in Kramer's Reaction Rate Theory,* P. Talkner and P. Hänggi, Eds., Kluwer, Dordrecht, 1995 p. 5.